Experimental Indicators of Accretion Processes in AGN (SMBHs)

Andreas Eckart

I.Physikalisches Institut der Universität zu Köln
Max-Planck-Institut für Radioastronomie, Bonn

SEVENTH FRAMEWORK PROGRAMME

STRONGGRAVITY
EU FP7-SPACE research project 312789 2013 - 2017

Max-Planck-Institut für Radioastronomie

I. Physikalisches Institut Universität zu Köln

St. Peterburg, Russian Federation, Sept 04-10

St. Petersburg Workshop 2016, Accretion Processes in Cosmic Sources

F. Peissker,
M. Valencia-S.,
M. Parsa,
M. Zajacek,
B. Shahzamanian,

EU FP7-SPACE project:
Strong Gravity
http://www.stronggravity.eu/

Experimental Indicators of Accretion Processes in AGN (SMBHs but not exclusively!)

i.e. observable activity indicators that allow to conclude on the nature of accretion

biased and incomplete view
each topic is worth a dedicated talk

Experimental Indicators of Accretion Processes in AGN

- Starformation and Black Hole Growth
- Relativistic radio jets
- NLR reverberation: response to long term variability
- BLR reverberation: short term response: BLR/size/map
- Variability and time lags: accretion disk size and structure

SgrA* as a special nearby case

- NIR polarization of SgrA* over the past ~10 years
- Radio/sub-mm single dish and VLBA monitoring
- Stability of the SgrA* system
- Monitoring the Dusty S-cluster Object:
  an accreting star (DSO alias G2) orbiting SgrA*
- DSO in NIR line emission as well as
- DSO in NIR continuum polarization

Overluminous host spheroids

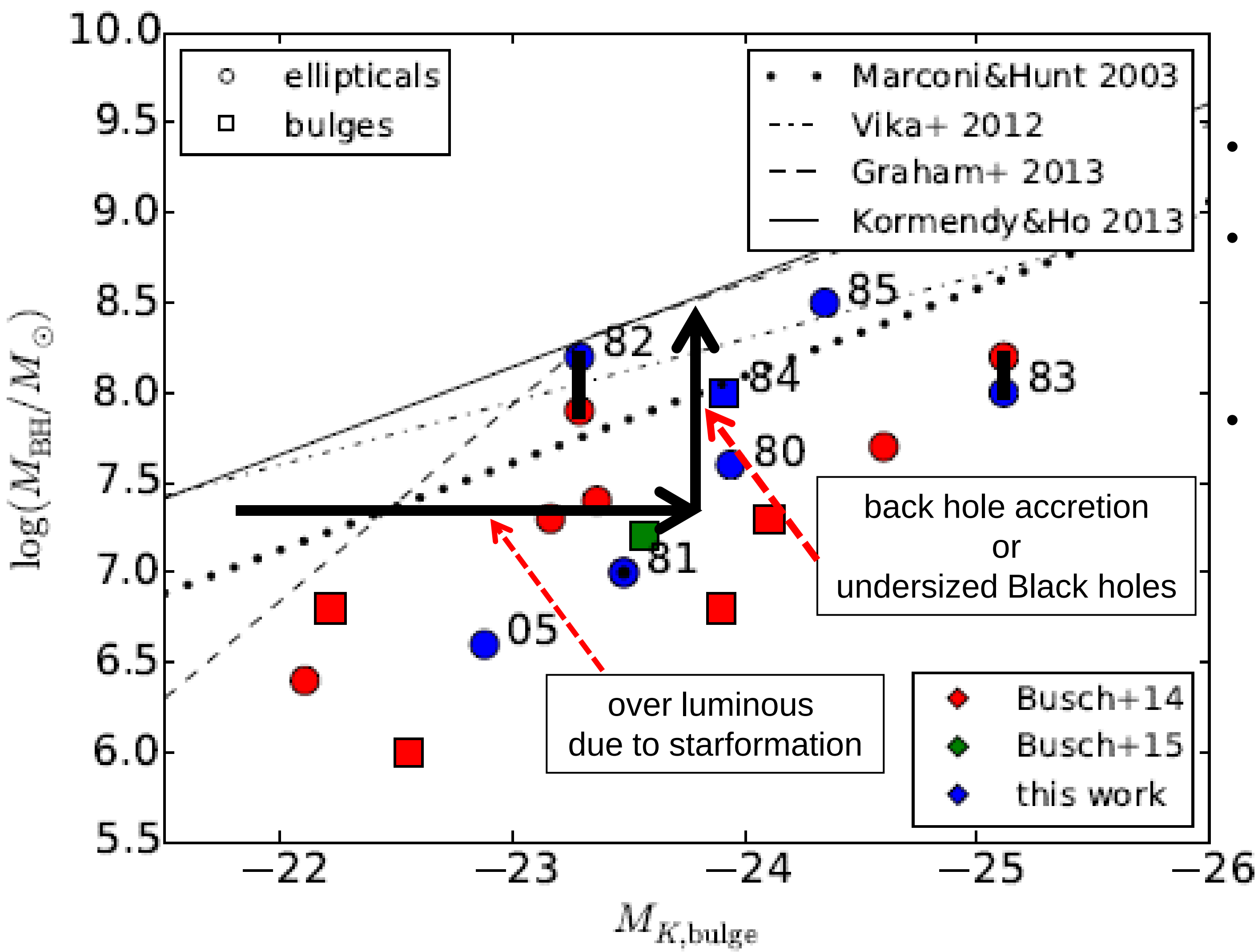

- Large H2 luminosity
- Indications for a large reservoir of molecular gas
- Indications for strong starformation

but:
bulge vs.
pseudobulge
discussion

Busch et al. A&A 561, 140, 2014

Merging: AGN accretion phases

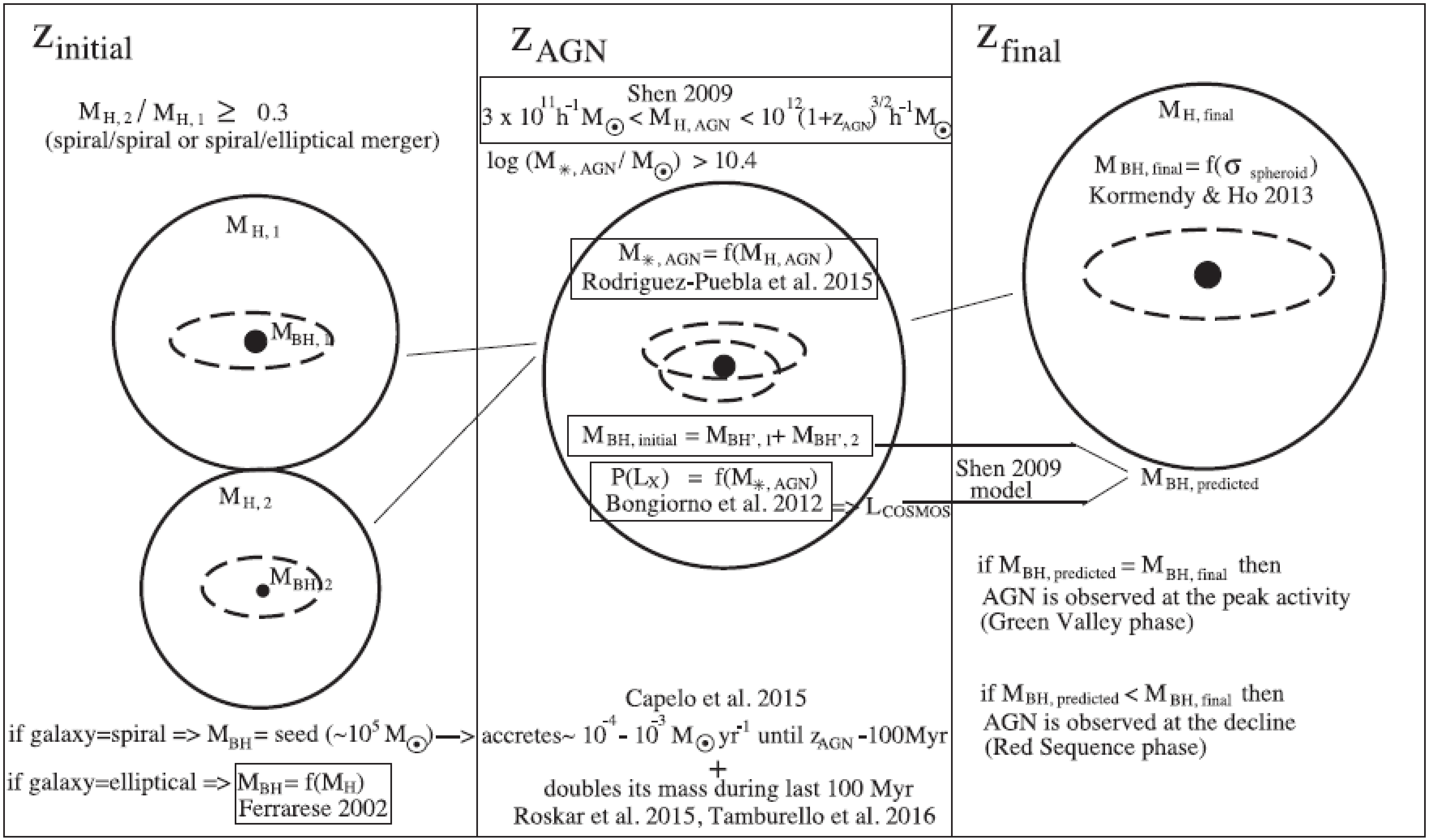

e.g. Micic et al., 2016, MNRAS 461, 3322

AGN accretion phases for field galaxies

peak between z=1 and 2

Jet speed vs. redshift: MOJAVE program

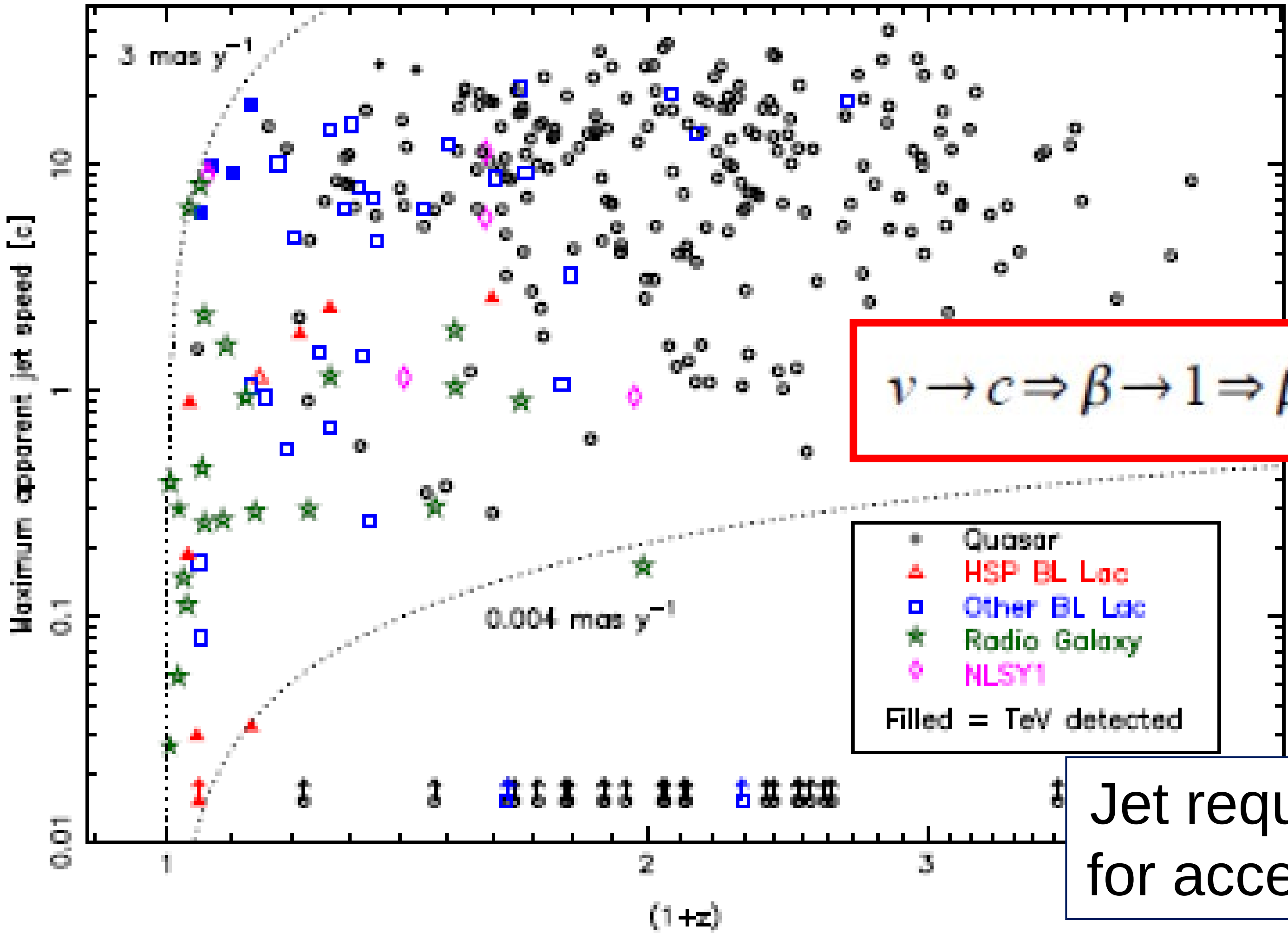

$$v \to c \Rightarrow \beta \to 1 \Rightarrow \beta_{t,max} \approx \gamma$$

Jet requires disk for acceleration?

274 AGN with 5 temporally separate measurements.

Lister et al. AJ 152, 12, 2016

Swerling Jets: The case of 1308+326

Precessing jets: variable geometry of accretion disk or environment

Britzen et al. 2016 submitted

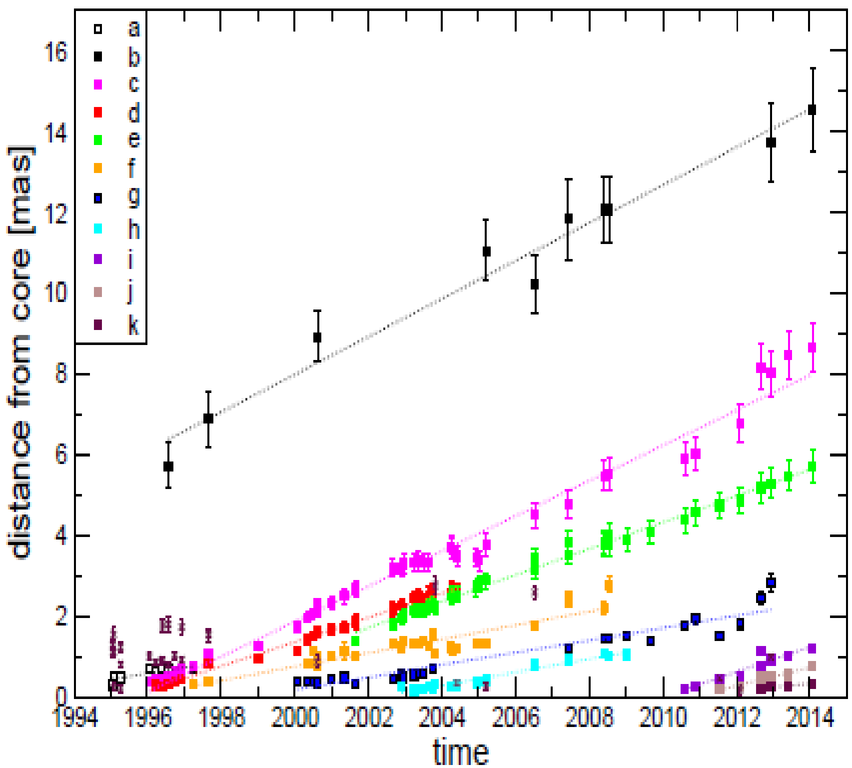

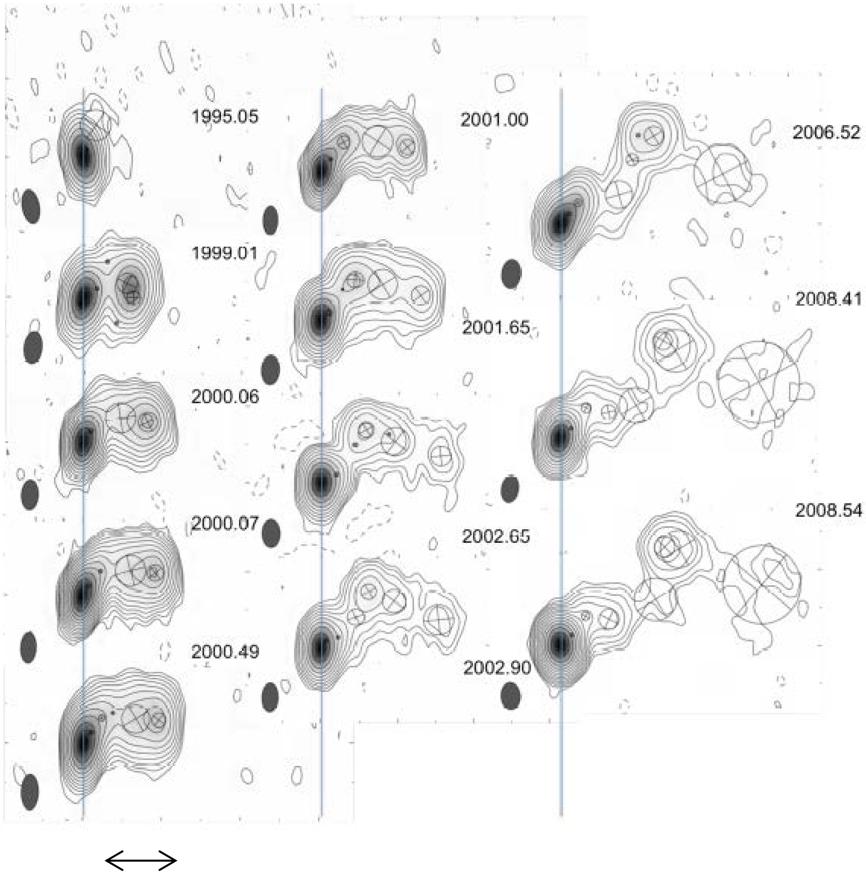

2 mas

Jet Mode change in 0735+178

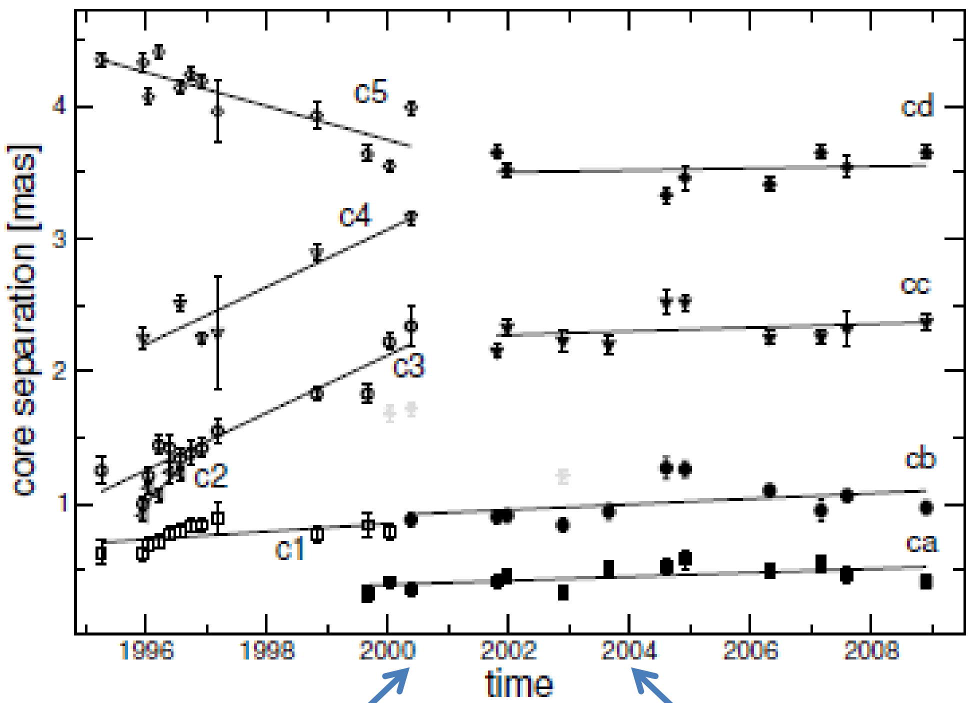

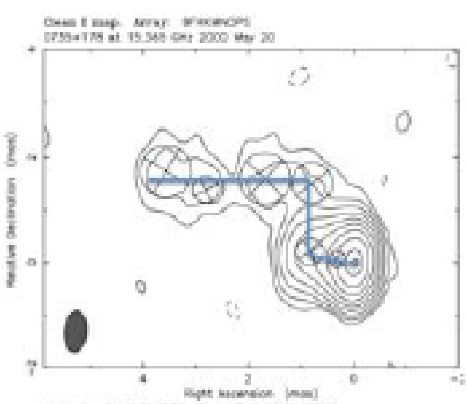

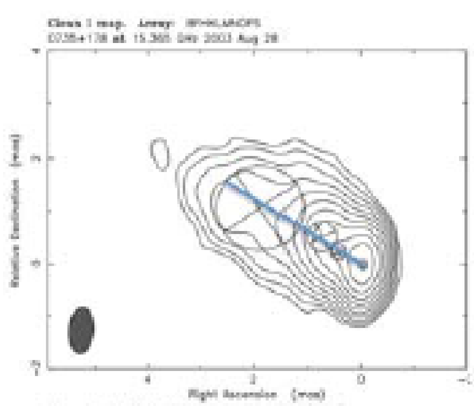

Mode changes jets: variable geometry of accretion disk or environment

VLBI jet-morphology and kinematics are correlated and switch between two modes (static – left and straight right).

Jet-Modes may be linked to accretion/acceleration modes.

Candidates for double black holes?

Britzen et al., AN 336, 471, 2015

Swerling Jets: The case of 1308+326

Possible magnetic field line structure

Blandford-Rees vs. Blandford–Znajek process for field i.e jet origin (production)

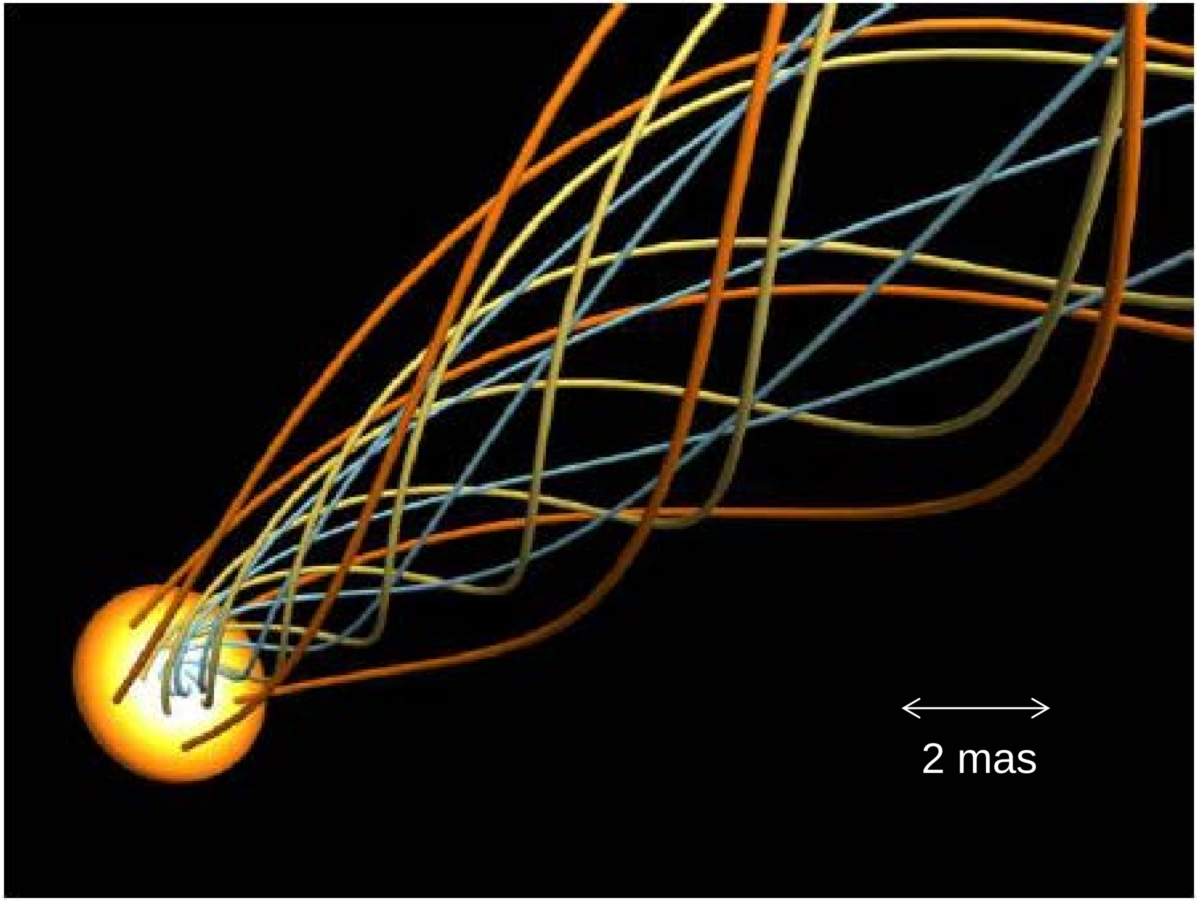

To give a better impression of the nature of components in 1308+326 we provide a schematic illustration.

Britzen et al. 2016 submitted

Unified Model

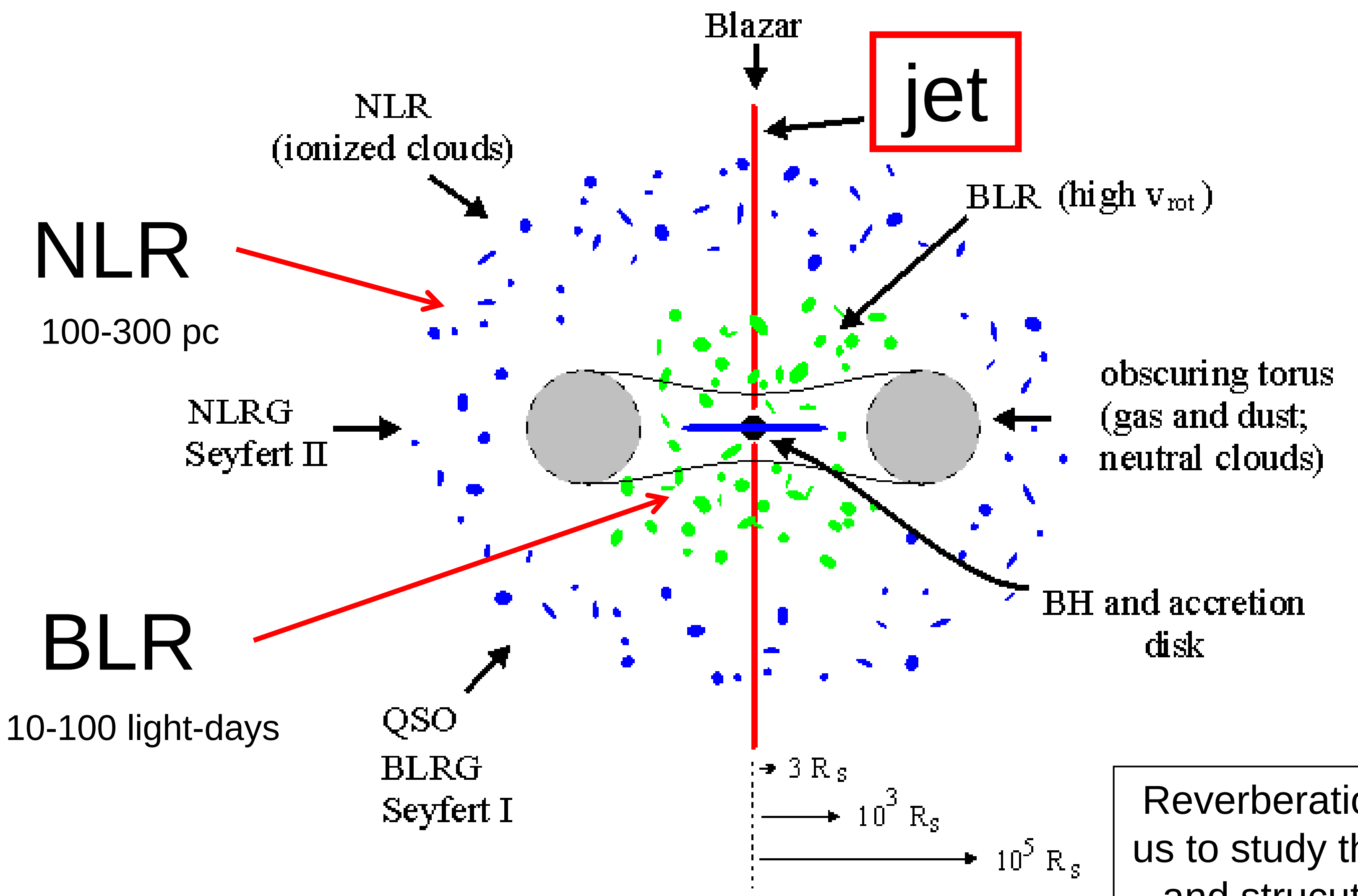

Reverberation allows us to study the activity and strucutre of the central region

astro.queensu.ca

Evidence from QSO spectra

Variability & spectrum : disk properties

Line variability & spectrum accretion properties

BBB

NLR/BLR

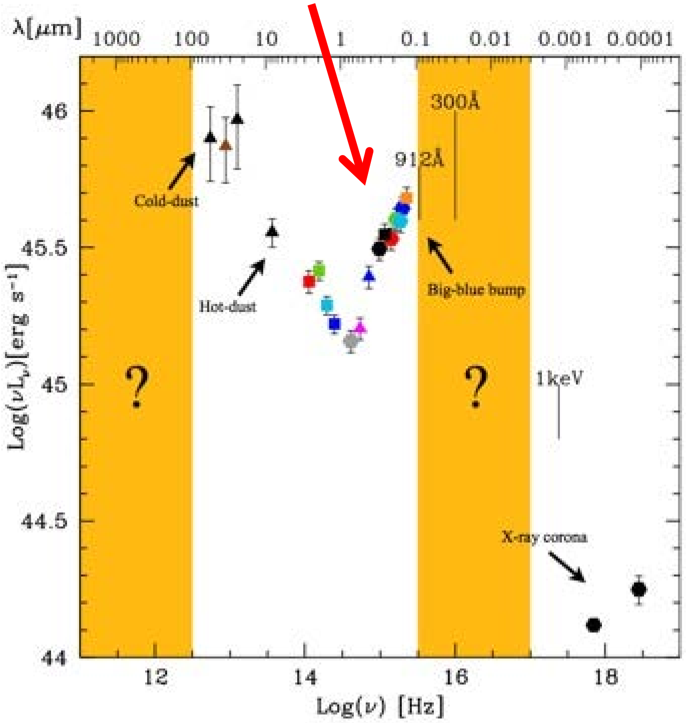

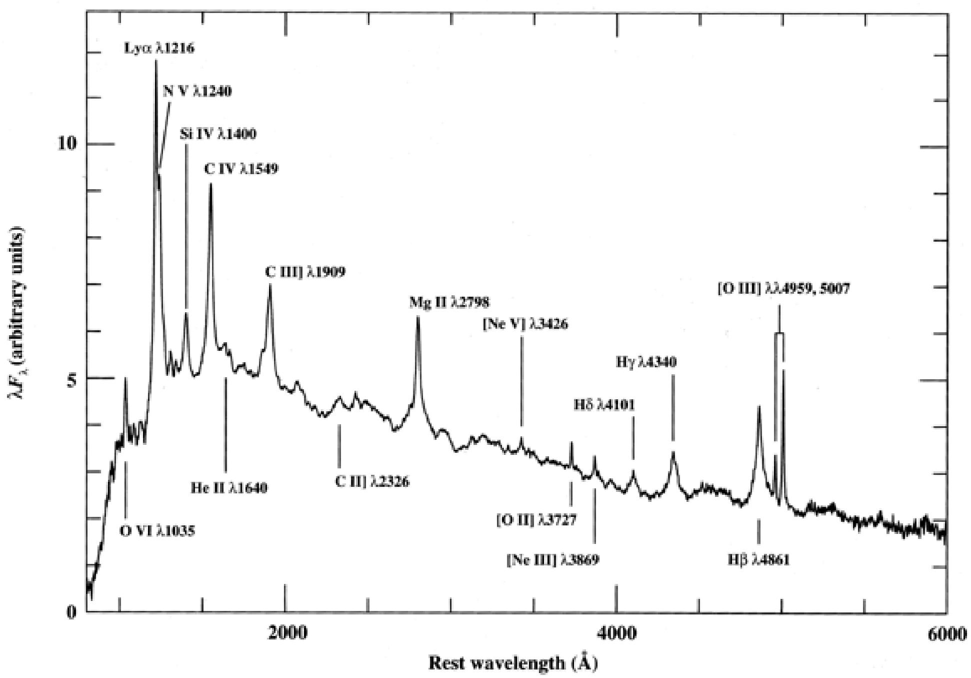

SED of a spectroscopically identified QSO from COSMOS. Lusso et al. (2011).

Mean QSO (Francis et al. 1991; courtesy of P. J. Francis and C. B. Foltz)

BLR Reverberation

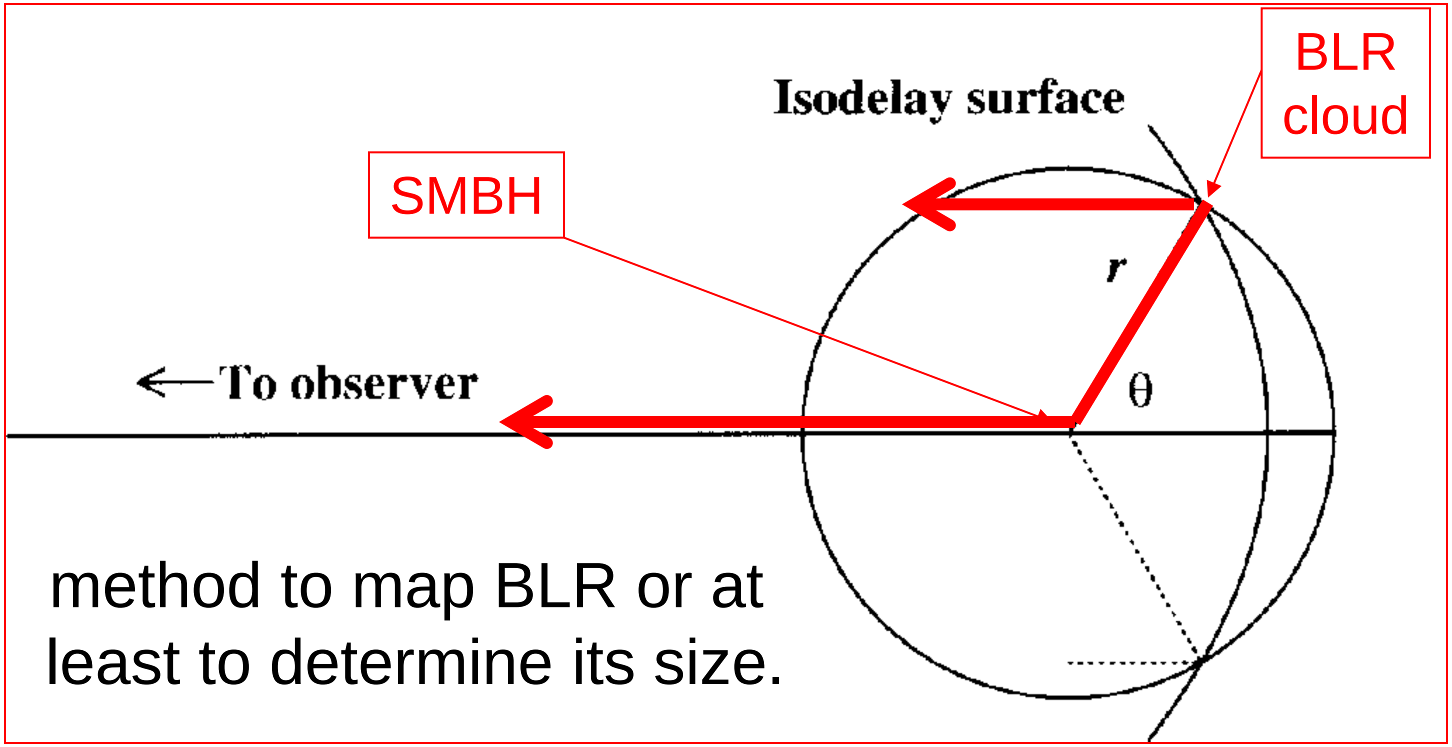

method to map BLR or at least to determine its size.

time delay: $\tau = (1+\cos\vartheta) r/c \longrightarrow d\tau = -r/c \sin(\vartheta) d\vartheta$

response function: $\Psi(\tau) d\vartheta = 2\pi\zeta\ r^2 \sin\vartheta d\vartheta$

(ζ surface emissivity)

$$\Psi(\tau) d\tau = \Psi(\vartheta) \left|\frac{d\vartheta}{d\tau}\right| d\tau = 2\pi\zeta r c d\tau$$

10-100 light-days

Disk size from opt./UV/X-ray time lags

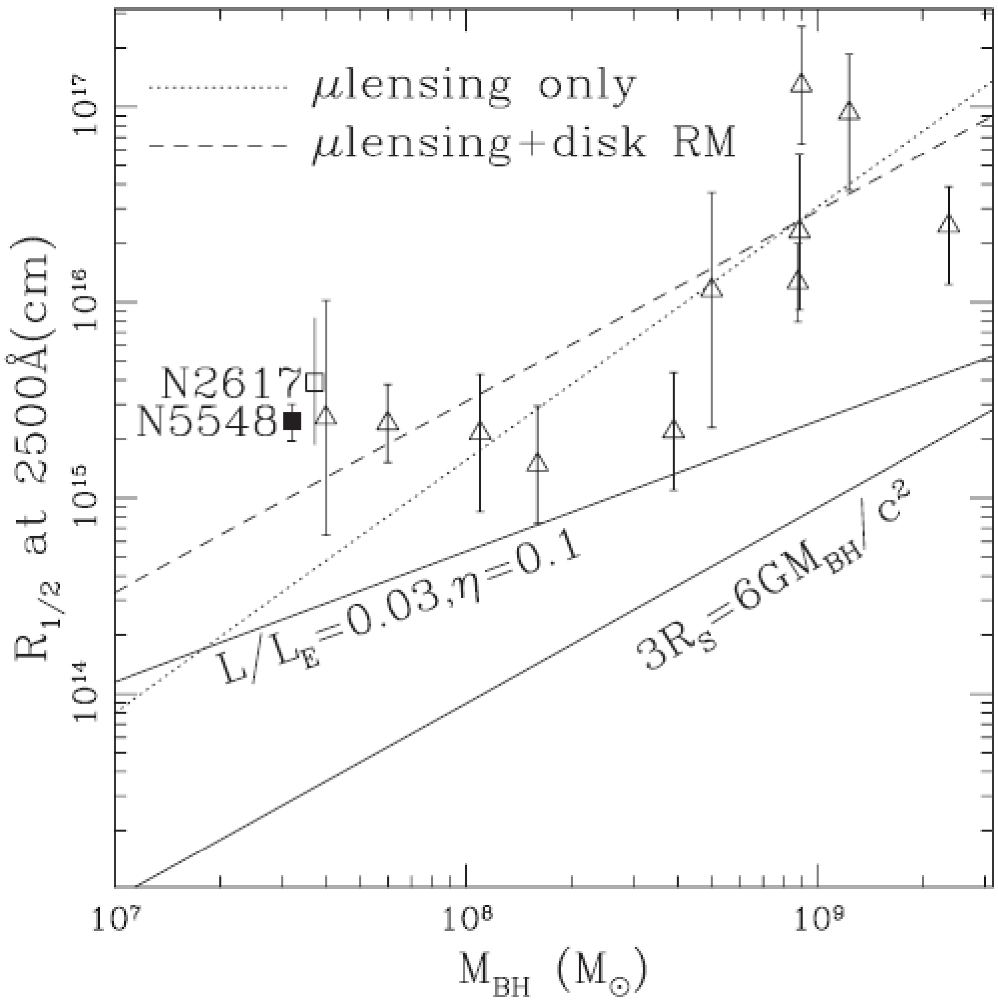

NGC5548

UV/opt lag 1-2 days:

$$\tau \propto \lambda^{4/3}$$

X-ray/UV lags
less pronounced

large disk size
0.35+-0.05 lt-days

(approximately consistent
with steady state
accretion disk theory)

Edelson et al. 2015, ApJ 806, 129

NLR Reverberation

Line and continuum variability in active galaxies

Y. E. Rashed,[1,2★] A. Eckart,[1,3★] M. Valencia-S.,[1] M. García-Marín,[1] G. Busch,[1]
J. Zuther,[1] M. Horrobin[1] and H. Zhou[4,5★]

2015, MNRAS 454, 291

18 sources; two to three epochs, with time intervals of 5 to 10 yr.

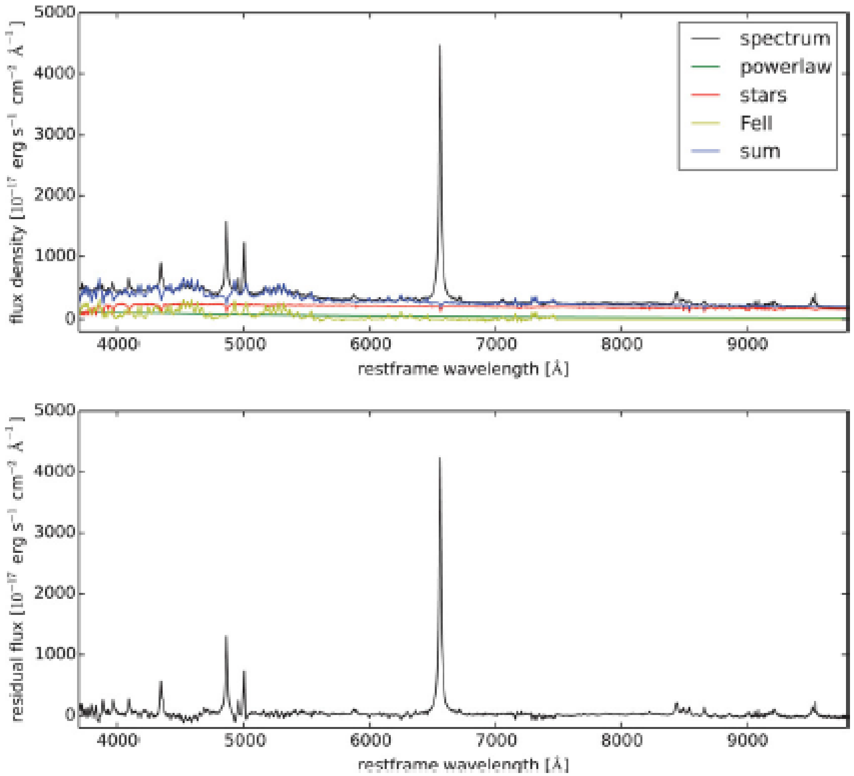

Figure 3. Results from the [Fe II] emission subtraction. The first plot shows the spectrum of J034740.18+010514.0 together with a fit of the [Fe II] emission (yellow). The second plot shows the spectrum after subtraction of the [Fe II] emission.

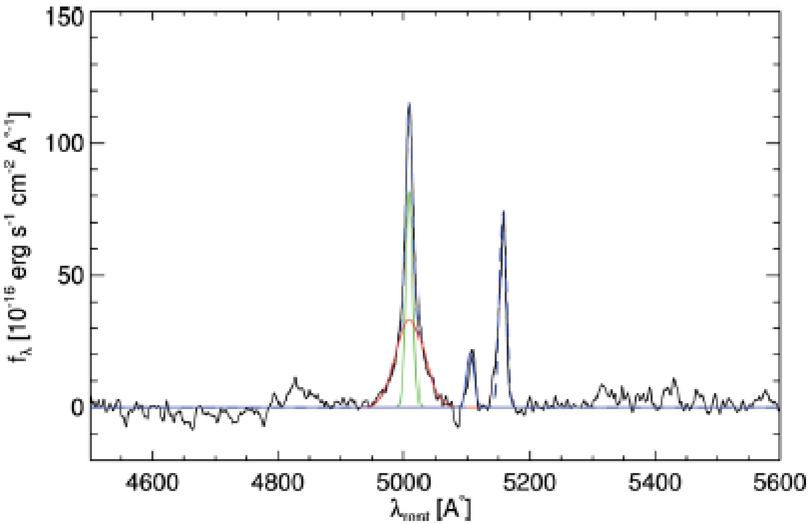

Figure 4. The fit of the Hβ and [O III] emission line complex with multiple Gaussian functions for J0347.

NLR Reverberation

continuum

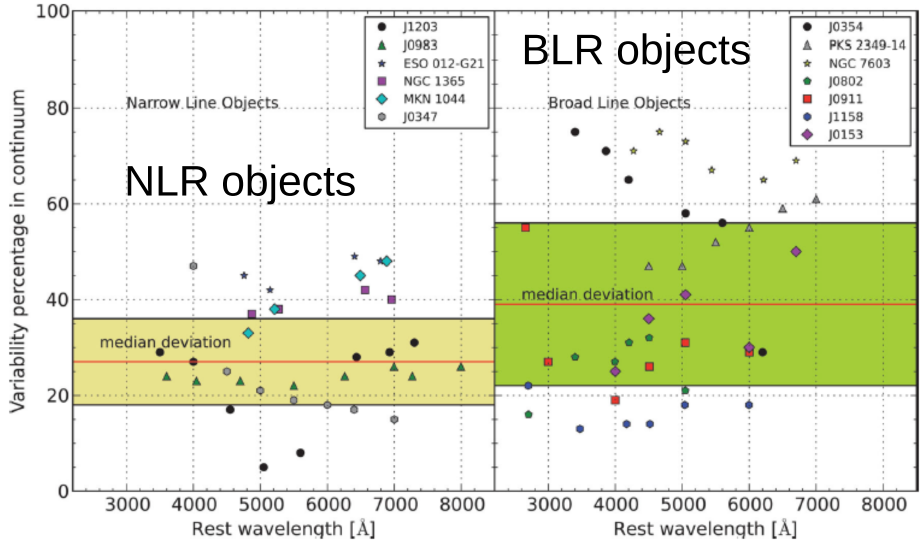

line emission

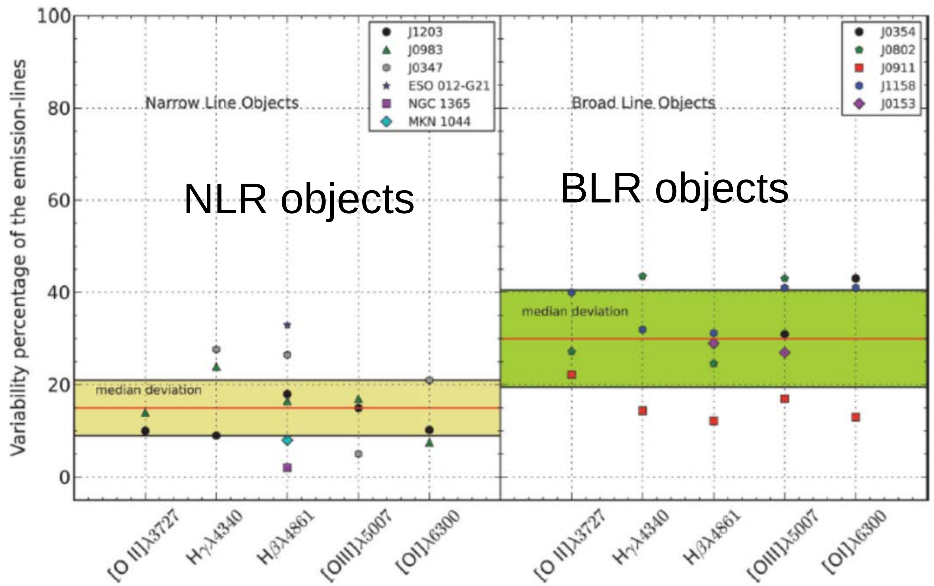

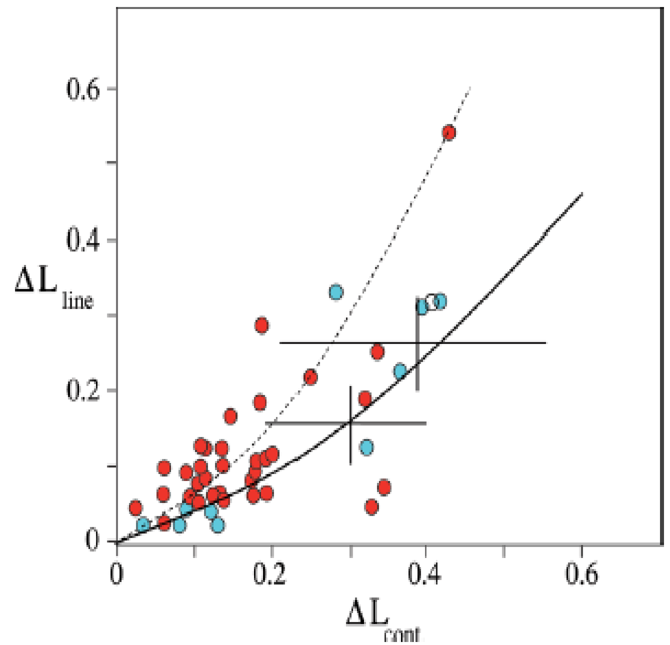

For otherwise constant accretion rate the total line variability reverberates in a similar way to the continuum variability with

Rashed et al. 2015, MNRAS 454, 291

NLR Reverberation

NLR is large but very compact i.e. brightness centraklly peaked

continuum radiation

$$L_{\rm cont} \propto M \frac{{\rm d}M}{{\rm d}t}.$$

$$\Delta L_{\rm cont} \propto \Delta M \frac{{\rm d}M}{{\rm d}t} + M \Delta \frac{{\rm d}M}{{\rm d}t}$$

$$\Delta L_{\rm cont} \propto \Delta M \frac{{\rm d}M}{{\rm d}t} \propto \frac{{\rm d}M}{{\rm d}t}.$$

const. rate

line radiation

Ac/Vc
~ sqrt(Lcont)

$$L_{\rm line} \propto \sqrt{M} (\frac{{\rm d}M}{{\rm d}t})^{3/2}.$$

$$\Delta L_{\rm line} \propto \frac{1}{2} M^{-\frac{1}{2}} \Delta M (\frac{{\rm d}M}{{\rm d}t})^{\frac{3}{2}} + M^{\frac{1}{2}} \frac{3}{2} (\frac{{\rm d}M}{{\rm d}t})^{\frac{1}{2}} (\Delta \frac{{\rm d}M}{{\rm d}t}).$$

$$\Delta L_{\rm line} \propto \Delta M (\frac{{\rm d}M}{{\rm d}t})^{3/2} \propto (\frac{{\rm d}M}{{\rm d}t})^{3/2}$$

Typically:
several 10 lyr
10-20 yrs

$$\Delta L_{\rm line} \propto (\Delta L_{\rm cont})^{3/2}$$

Typically:
NLR large but very centrally peaked

Rashed et al. 2015, MNRAS 454, 291

NLR Reverberation

continuum radiation

$$L_{\rm cont} \propto M \frac{{\rm d}M}{{\rm d}t}.$$

$$\Delta L_{\rm cont} \propto \Delta M \frac{{\rm d}M}{{\rm d}t} + M \,\Delta \frac{{\rm d}M}{{\rm d}t}$$

$$\Delta L_{\rm cont} \propto \Delta M \frac{{\rm d}M}{{\rm d}t} \propto \frac{{\rm d}M}{{\rm d}t}.$$

line radiation

$$L_{\rm line} \propto \sqrt{M} \left(\frac{{\rm d}M}{{\rm d}t}\right)^{3/2}.$$

$$\Delta L_{\rm line} \propto \frac{1}{2} M^{-\frac{1}{2}} \Delta M \left(\frac{{\rm d}M}{{\rm d}t}\right)^{\frac{3}{2}} + M^{\frac{1}{2}} \frac{3}{2} \left(\frac{{\rm d}M}{{\rm d}t}\right)^{\frac{1}{2}} \left(\Delta \frac{{\rm d}M}{{\rm d}t}\right).$$

$$\Delta L_{\rm line} \propto \Delta M \left(\frac{{\rm d}M}{{\rm d}t}\right)^{3/2} \propto \left(\frac{{\rm d}M}{{\rm d}t}\right)^{3/2}$$

$$\boxed{\Delta L_{\rm line} \propto (\Delta L_{\rm cont})^{3/2}}$$

Structure of the accretion disk

CASE 1: low accretion rate
high opacity

$$\dot{M}/\dot{M}_E \lesssim 0.1$$

thin accretion disk
compared to diameter
efficiency: $\eta \approx 0.1$

plus advection
dominated accretion
for LLAGN

$$\dot{M} << \dot{M}_E$$

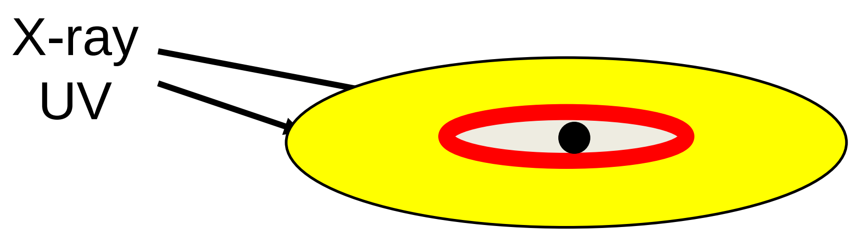

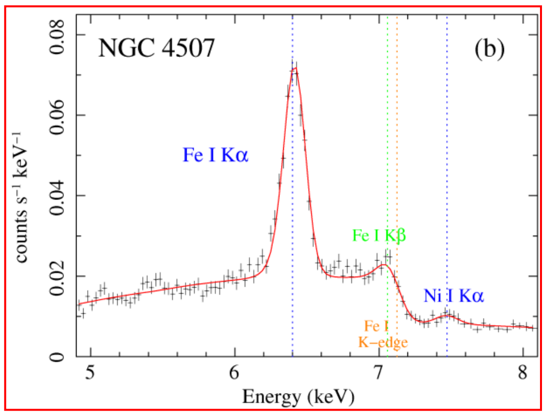

Suzaku data

$\gg$

CASE 2: high accretion rate
radiation heats disk
disk inflates and cools
at larger radii, i.e.
radiation becomes
inefficient.

$$\dot{M}/\dot{M}_E \gg 1$$

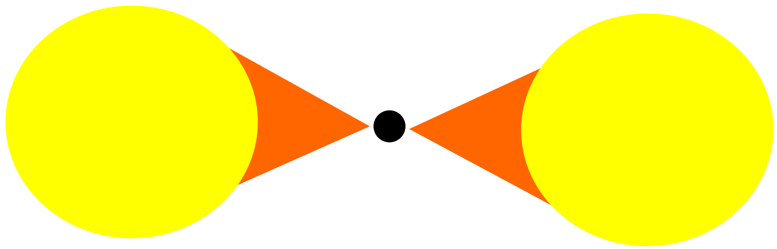

looks like a
10**4 K
young star

SgrA* as an extreme LLAGN Nucleus

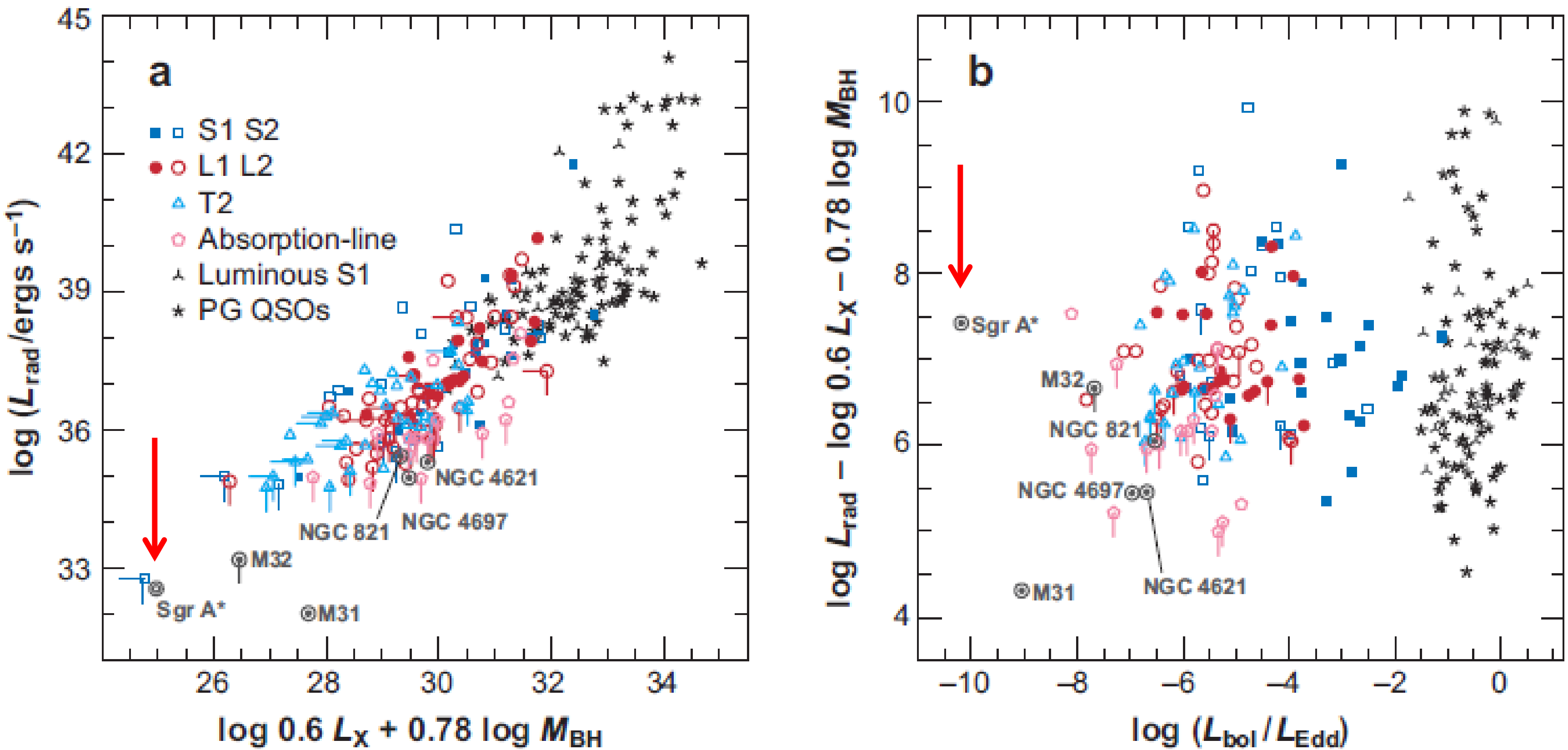

Ho 2008: Fundamental plane correlation among core radio luminosity, X-ray (a) luminosity, and BH mass. (*b*) Deviations from the fundamental plane as a function of Eddington ratio.

SgrA* is accreting in an advection dominated mode, else ist luminosity would be than 10^7 times higher

SgrA* as a special nearby case

- NIR polarization of SgrA* over the past ~10 years
- Stability of the SgrA* system
- Radio/sub-mm single dish and VLBA monitoring
- Monitoring the Dusty S-cluster Object:
  an accreting star (DSO alias G2) orbiting SgrA*
- DSO in NIR line emission as well as
- DSO in NIR continuum polarization

SgrA* and its Environment

Orbits of High Velocity Stars
in the Central Arcsecond

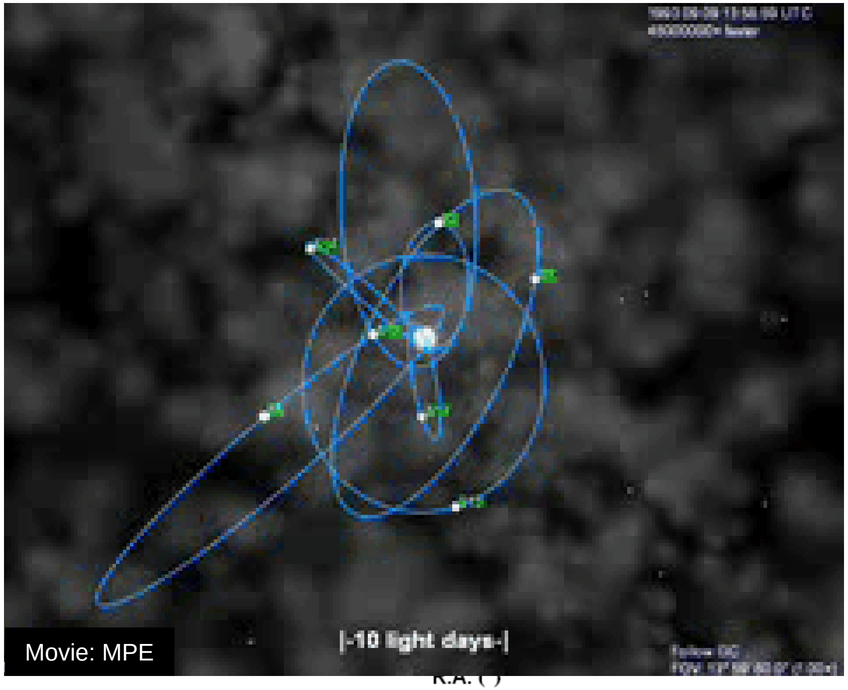

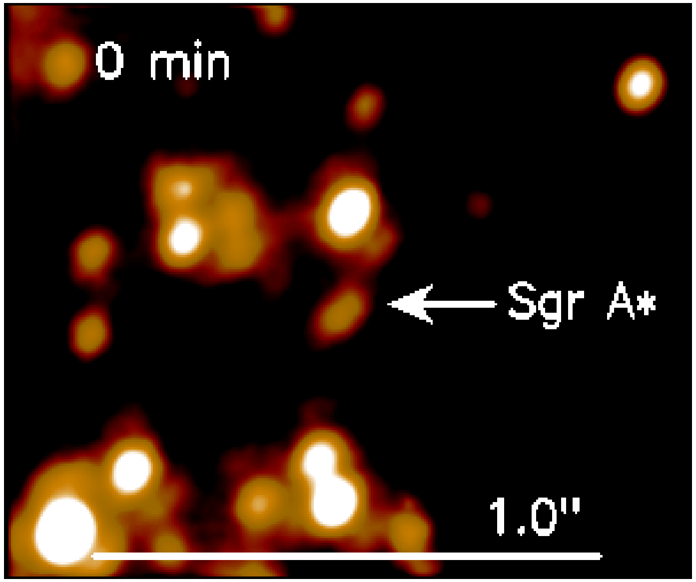

Eckart & Genzel 1996/1997 (first proper motions)
Eckart+2002 (S2 is bound; first elements)
Schödel+ 2002, 2003 (first detailed elements)
Ghez+ 2003 (detailed elements)
Eisenhauer+ 2005, Gillessen+ 2009
(improving orbital elements)
Rubilar & Eckart 2001, Sabha+ 2012, Zucker+2006
(exploring the relativistic character of orbits)

~4 million solar masses
at a distance of
~8+-0.3 kpc

SgrA* - Stable Geometry and Accretion

SgrA* is a stable system

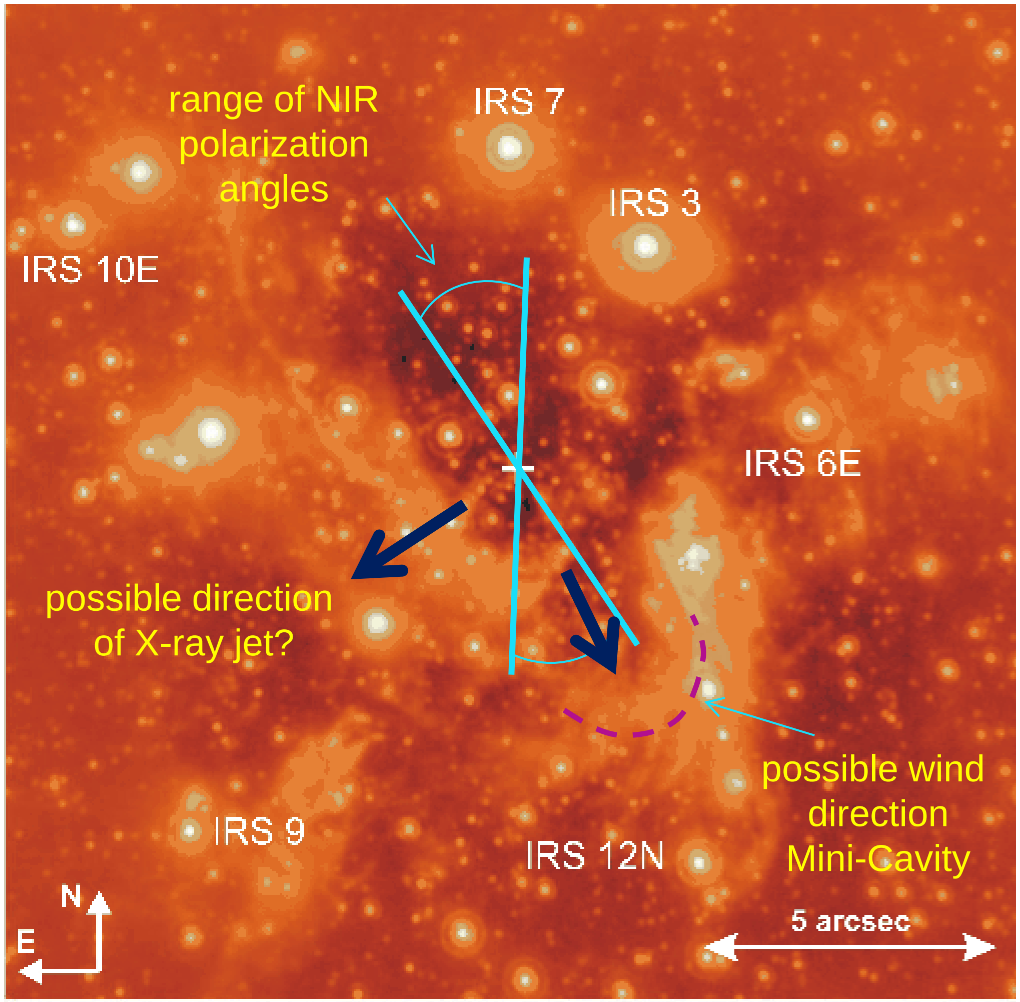

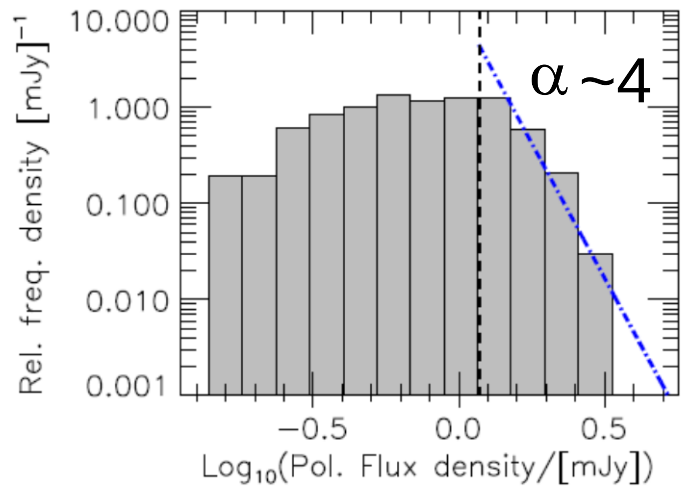

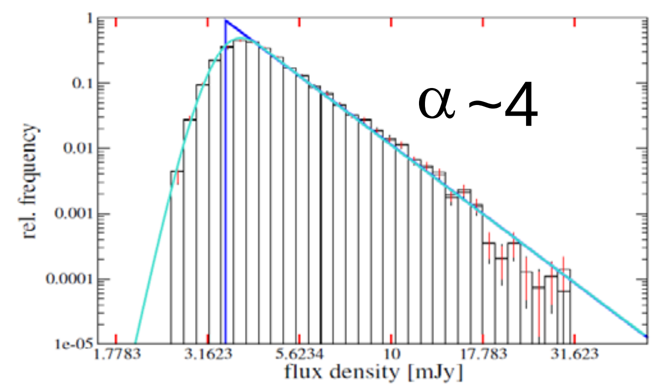

SgrA* 345GHz/100GHz varibility

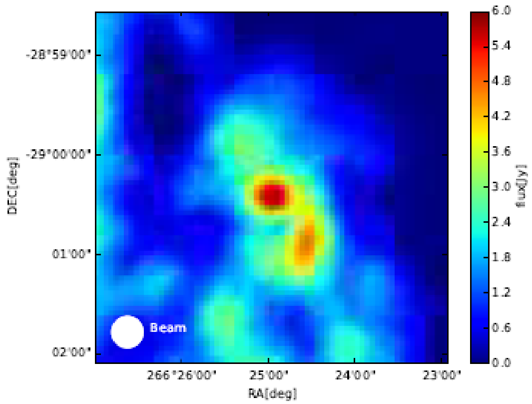

Fig. 1. A single measurement map of the GC from 2009-05-17T04:19:58, the extended submm emission from the surroundings of Sgr A* (CNR and Minispiral) dominate the data.

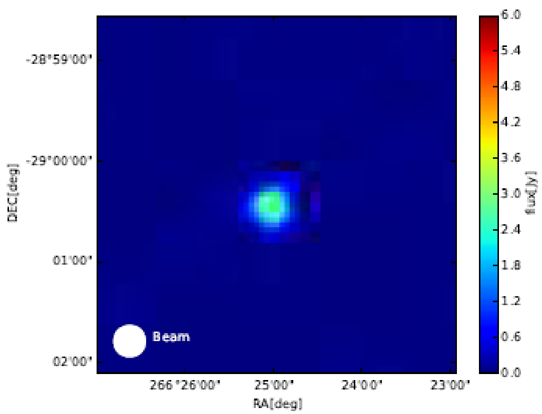

Fig. 2. A single measurement map of the GC from 2009-05-17T04:19:58 with subtracted background. The remaining point-like source represents the submm emission from Sgr A* itself.

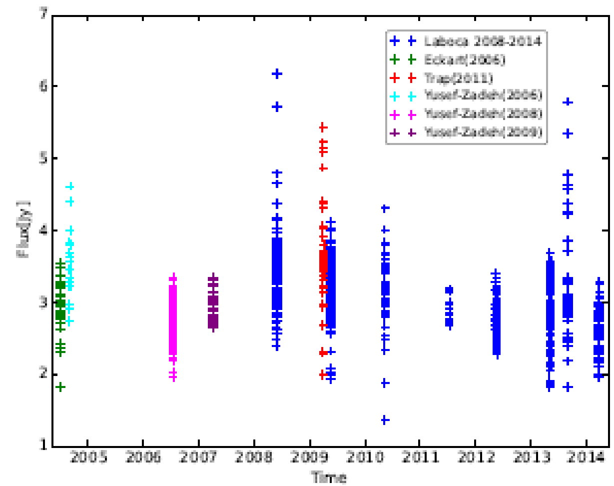

Fig. 3. All light curves obtained between 2004 and 2014. This plot contains both the LABOCA data (blue markers) and the literature data (other colors).

Borkar et al. MNRAS 2016
Subroweit et al. 2016

SgrA* 345GHz/100GHz varibility

Borkar et al. MNRAS 2016
Subroweit et al. 2016

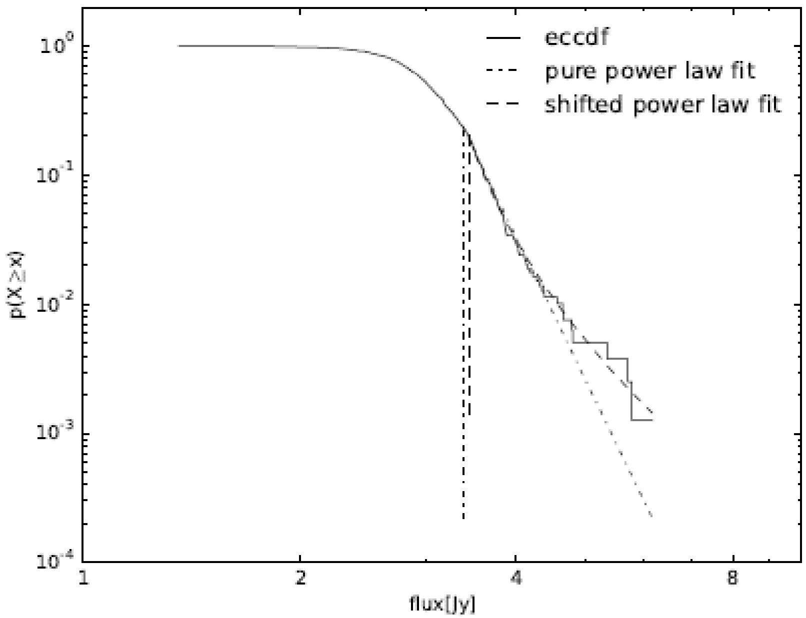

345 GHz LABOCA

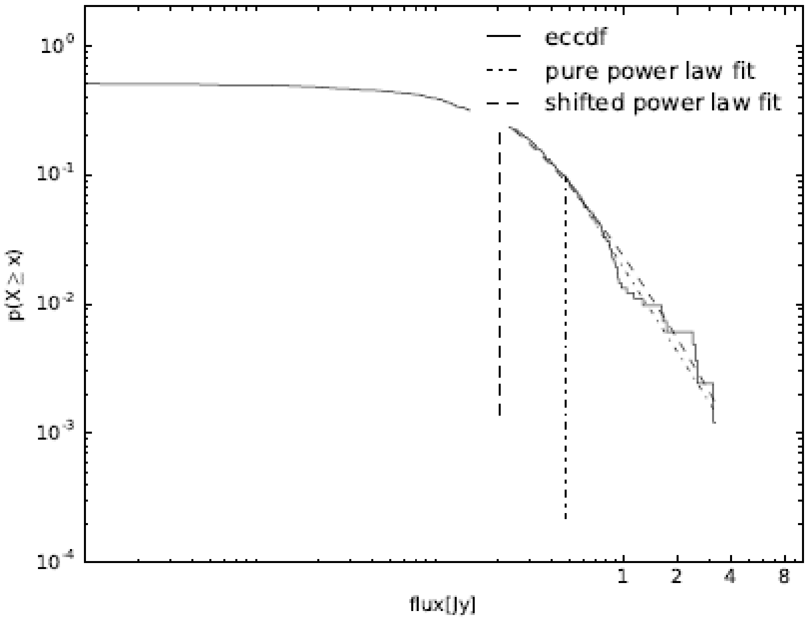

100 GHz ATCA

$$S(100\ \mathrm{GHz}, t) \sim S(\nu_0 = 100\ \mathrm{GHz}, t) + S_{\mathrm{adiab}}(\nu_0 > 100\ \mathrm{GHz}, t)$$

Adiabatic Expansion in SgrA*

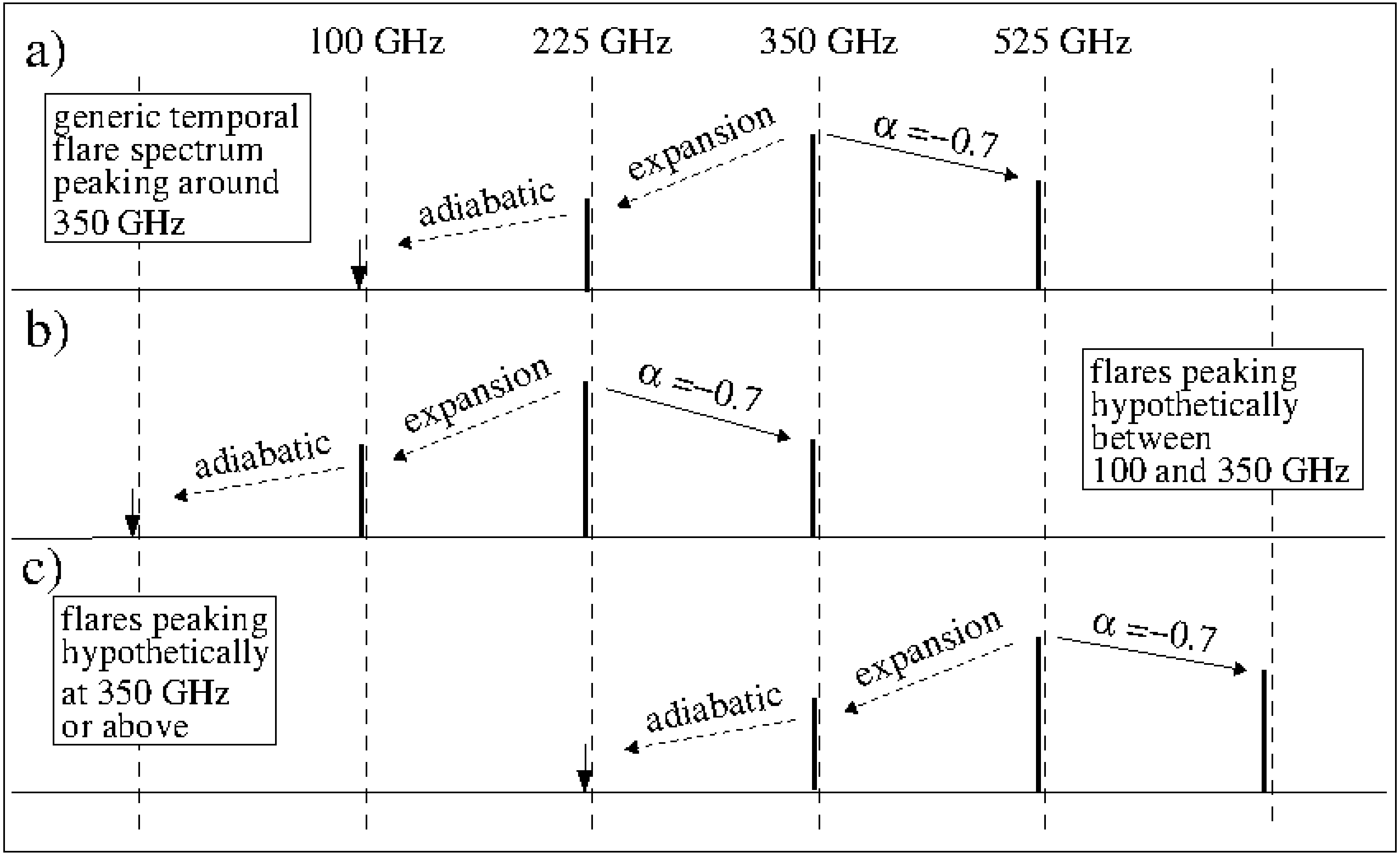

Subroweit et al. 2016 submitted

SgrA* 345GHz/100GHz varibility

Borkar et al. MNRAS 2016
Subroweit et al. 2016

SgrA* peaks around 350 GHz

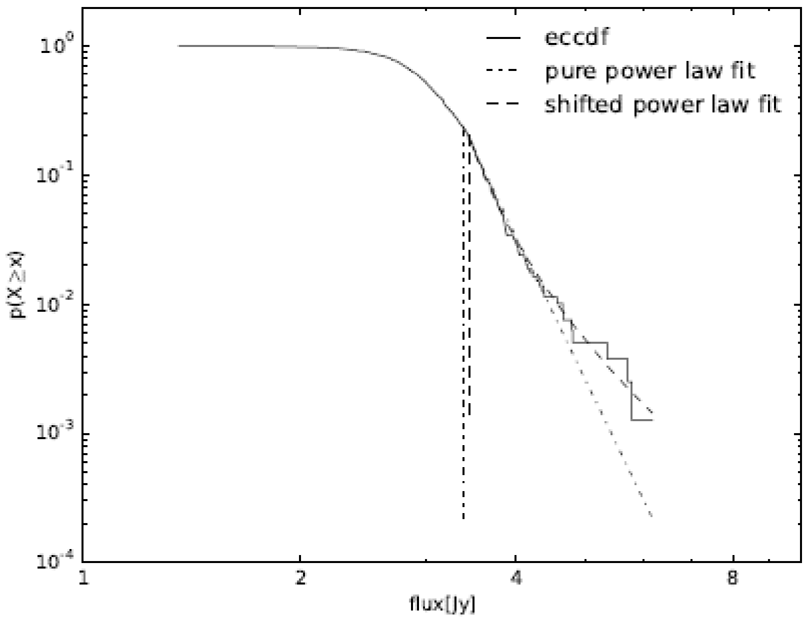

345 GHz LABOCA

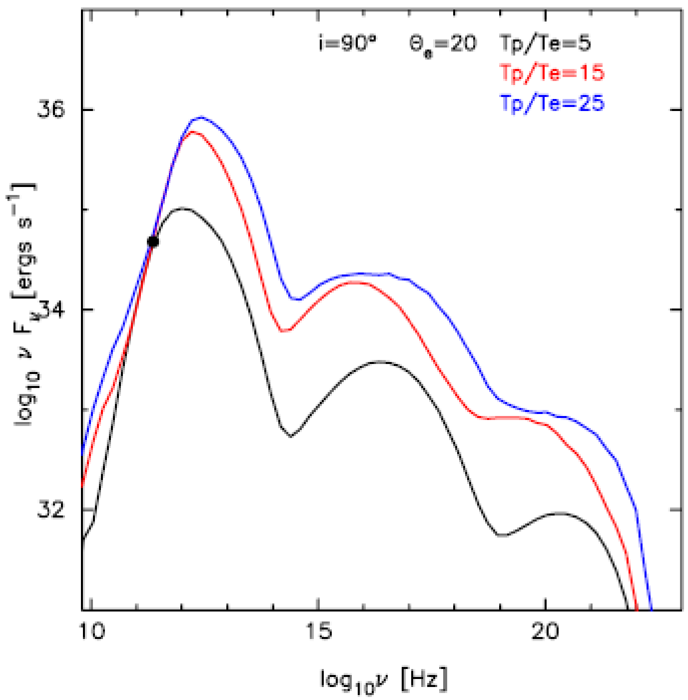

$$S(100\ \mathrm{GHz}, t) \sim S(\nu_0 = 100\ \mathrm{GHz}, t) + S_{\mathrm{adiab}}(\nu_0 > 100\ \mathrm{GHz}, t)$$

Adiabatic Expansion in SgrA*

$$\nu_m = \nu_{m0}\left(\frac{R(t)}{R_0}\right)^{-(4p+6)/(p+4)}$$

van der Laan (1966)

$$R(t) = v_{\rm exp} t + R_0$$

$$p = 1 - 2\alpha_{\rm sync} \sim 2.4,$$

$$\frac{R(t)}{R_0} \sim \left(\frac{\nu_m}{\nu_{m0}}\right)^{-1/2.44} \sim \left(\frac{100\,\mathrm{GHz}}{350\,\mathrm{GHz}}\right)^{-1/2.44} \approx 1.67$$

starting at ~1 Rs

$$v_{\rm exp} \times 0.5\,\mathrm{h} \sim 0.67\,R_S.$$

$$v_{\rm exp} \sim 0.01\,\mathrm{c}$$

Subroweit et al. 2016 submitted

Jet vs. Core Luminosity in SgrA*

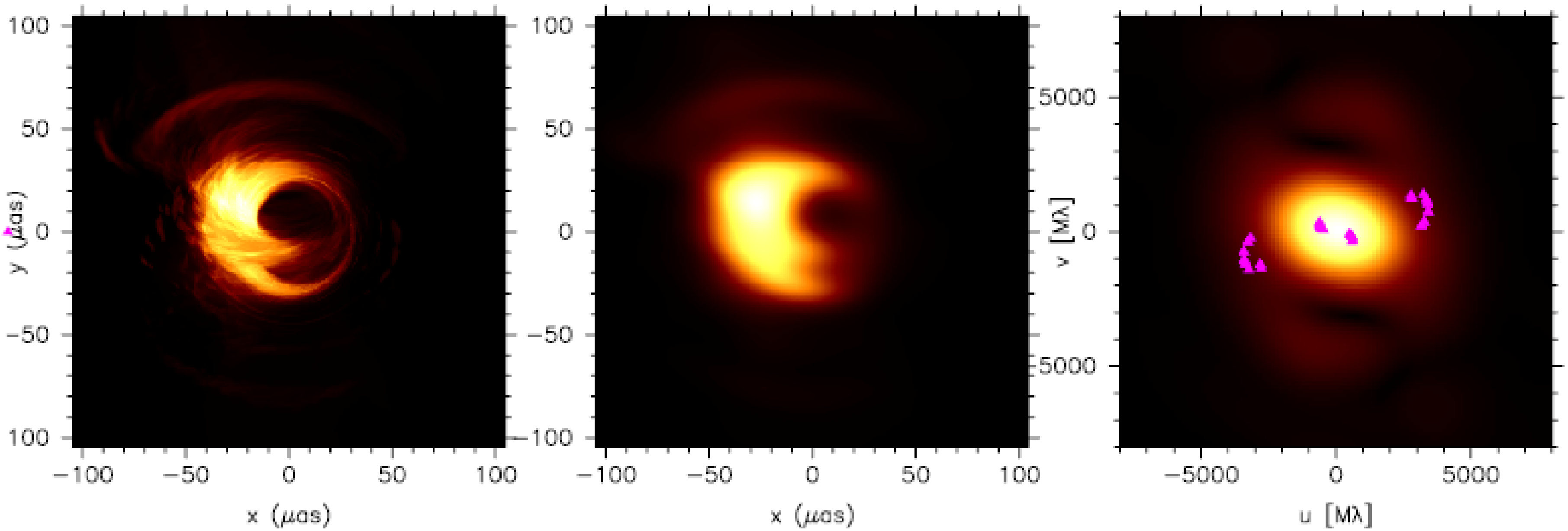

Fig. 8. Intrinsic image, scatter-broadened image, and visibility amplitude distribution for model 24 at $\lambda = 1.3$ mm. Images are time-averaged (over $\Delta t \approx 3$ h) and the color intensity indicates the intensity of radiation normalized to unity (linear scale). The visibility amplitudes are in units of Jansky. The visibility $u - v$ tracks are from Fish et al. (2011).

Moscibrodzka et al., A&A 570, A7, 2014

Jet vs. Core Luminosity in SgrA*

200x200 Rg | 20x20 Rg

$$\left(\left(\frac{T_p}{T_e}\right)_{disk}, \Theta_{e,jet}\right)$$

(5,20)

(15,20)

(25,20)

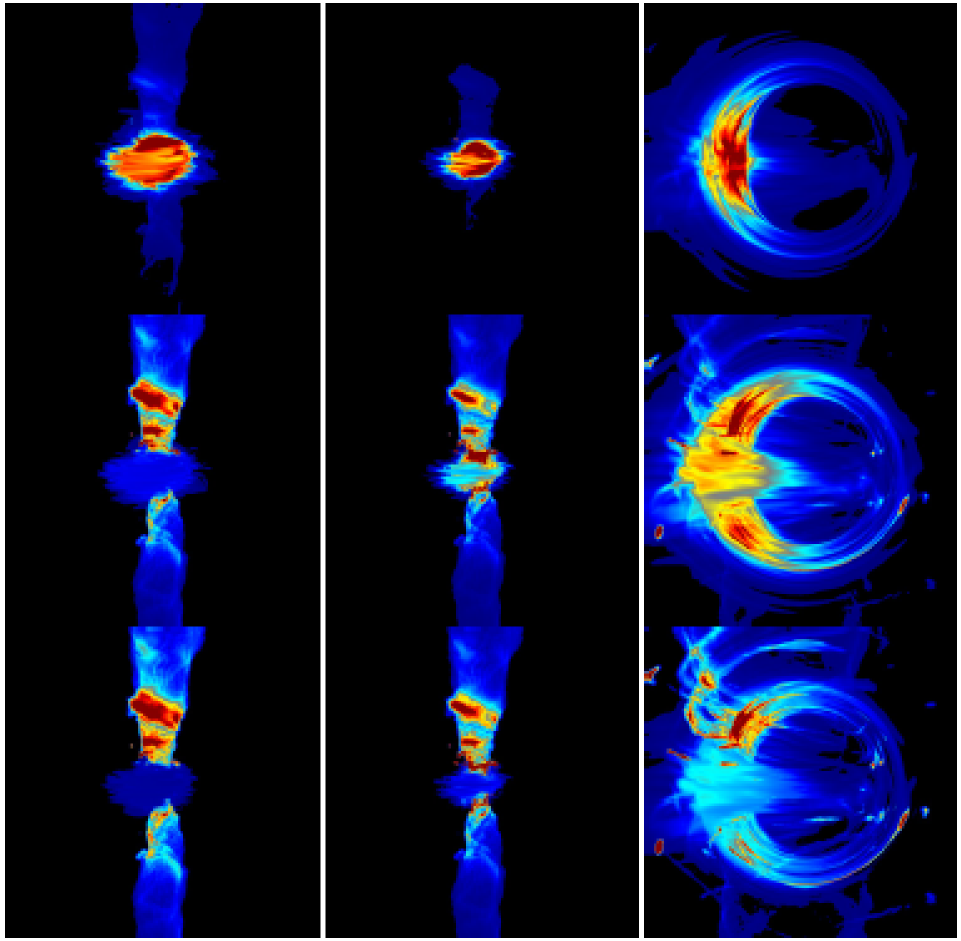

13 mm | 7 mm | 1.3 mm

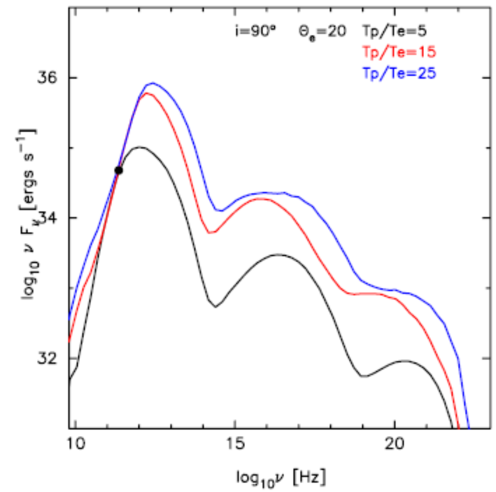

Jet:
const. E-Temp.

$$\frac{k_b T_e}{m_e c^2} = \Theta_{e,j} = \text{const.}$$

Disk: proton
e-Temp. ratio

$$\frac{k_b T_e}{m_e c^2} = \left(\frac{k_b T_p}{\mu m_p}\right)\left(\frac{m_p}{m_e}\right)\frac{1}{(T_p/T_e)_{disk}}$$

Moscibrodzka et al., A&A 570, A7, 2014

Nature of some SgrA* radio flares

7 mm VLBA

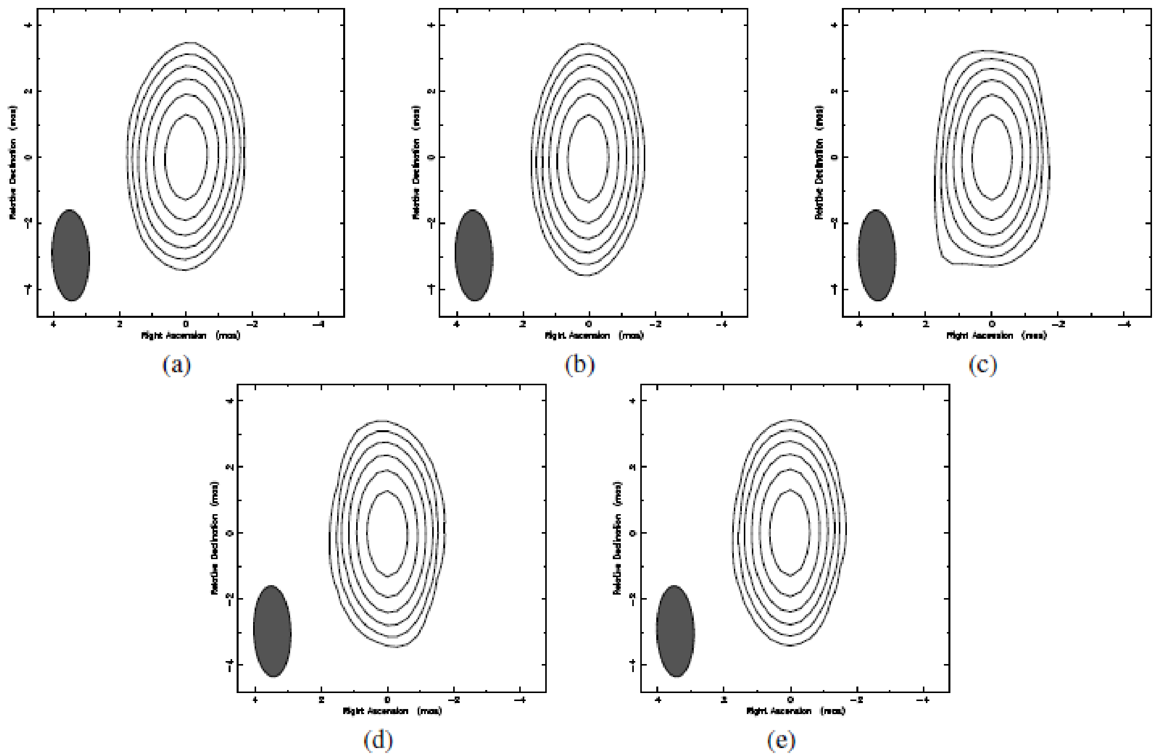

Fig. 5: 2 hour LCP maps of Sgr A* observed on May 17 2012. (a) May 17 6-8h. (b) May 17 7-9h. (c) May 17 8-10h. (d) May 17 9-11h. (e) May 17 10-12h. Summarized map parameters can be found in table 2.

Rauch et al. 2016

Nature of some SgrA* radio flares

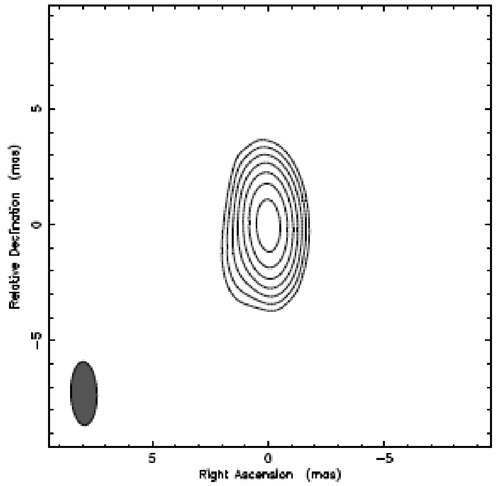

Fig. 7: RCP map of Sgr A* on May 17 2012 (8-10h UT). The map was convolved with a beam of 2.74×1.12 at 1.76°. Contour levels are 1, 2, 4, 8, 16, 32 and 64% of the peak flux density of 1.5 Jy/beam.

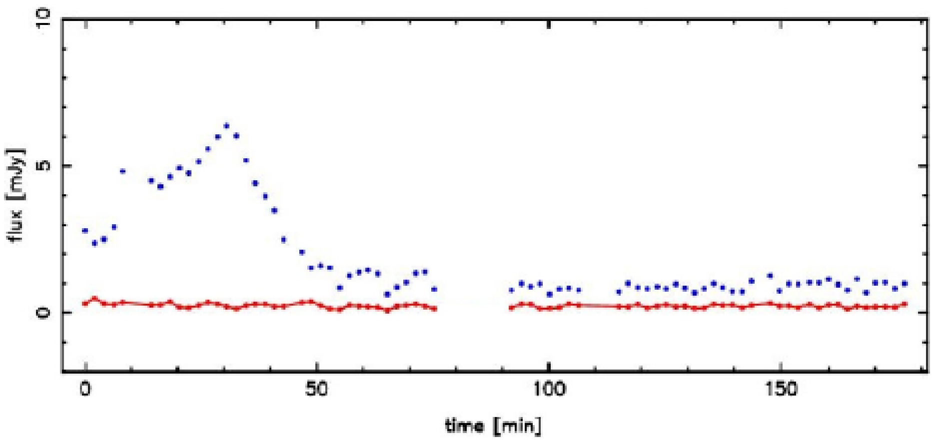

Fig. 3: NIR K_s-band (2.2 μm) light curve of Sgr A* observed in polarimetry mode on 17 May 2012. The light curve shown is produced by combining pairs of orthogonal polarization channels: 0° and 90° (taken from Shahzamanian et al. (2015)). Observations started at 4:55 AM UT.

Central component of 1.55 Jy secondary component of 0.02 Jy at 1.5 mas and 140 deg. E-N with a 4 hout delay relativ to the NIR flare

Bower et al. (2014) report major axis sizes of Sgr A* as an elliptical Gausssian of 35.4 × 12.6 R_S at an position angle of 95° east of north. Which is much lower than the discussed source morphology due to a secondary component of 0.02 Jy at 1.8±0.4 mas at 140° east of north.

Rauch et al. 2016

See also ‚Asyummetric structure in SgrA* …' Brinkerink et al. 2016, MNRAS 462, 1382 'speckle transfer function?'

Monitoring the Orbit of the DSO

Eckart, A., et al., 2014 ATel
Valencia-S., M., et al. 2015, ApJ 800, 125
Zajacek, Karas, Eckart, 2013, A&A 565, 17
Eckart et al. 2013, A&A 551, 18
Peissker et al. 2016 in prep

Accretion of matter
(from ist shell or disk
[or companion]?)
onto a
Galactic Center star?!

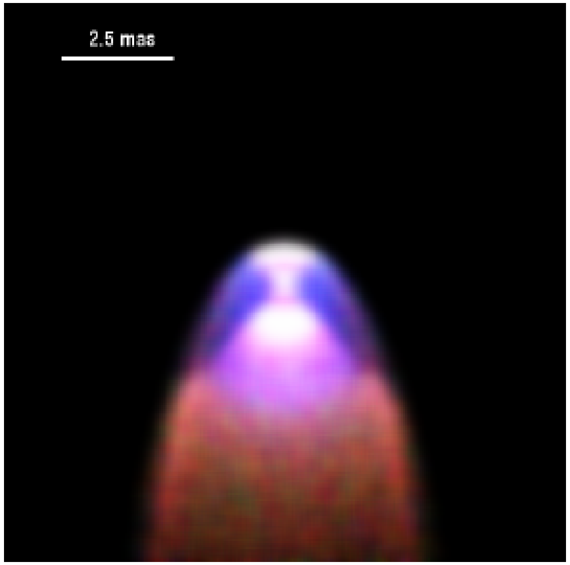

Fig. 9. The RGB image of the source model of the DSO. The explanation is in the text.

Dusty S-cluster Object(DSO/G2)

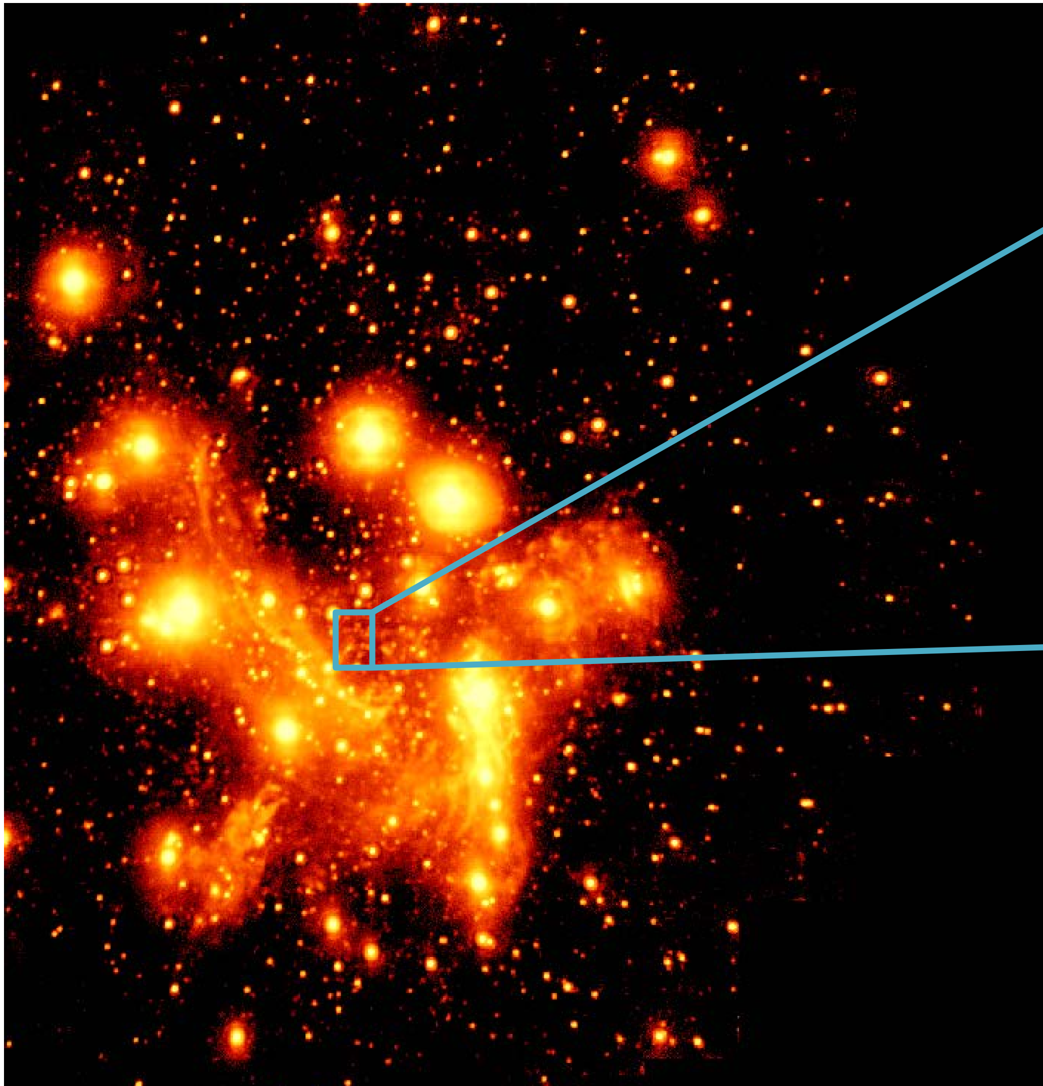

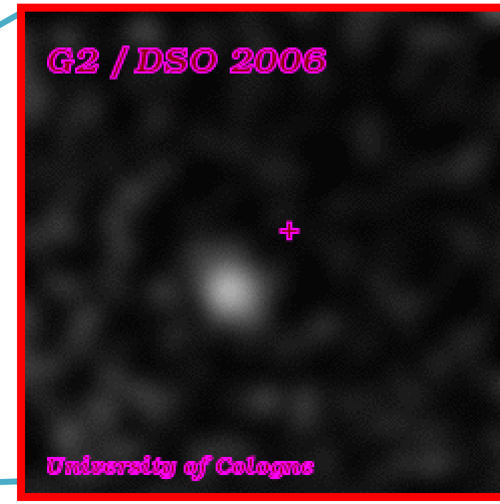

Gillessen et al. 2012,2013a,b; Eckart et al. 2013a,b; Phifer et al. 2013; Pfuhl et al. 2014; Burkert et al. 2012; Schartmann et al. 2012; Witzel et al. 2014; Valencia-S. et al. 2015; Zajacek, Karas, Eckart 2015… ...

GC in L-Band. Courtesy: N. Sabha/Uni. of Cologne

DSO/G2 Approaching SgrA*

Gillessen et al. 2012/13
Burkert et al. 2012,
Schartmann et al. 2012

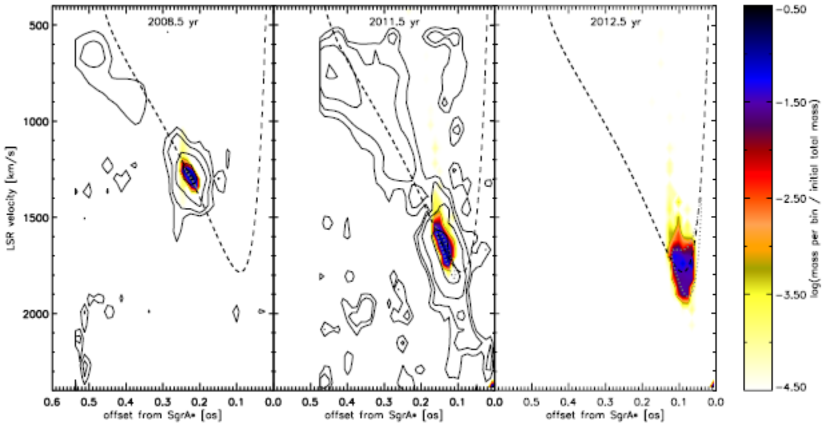

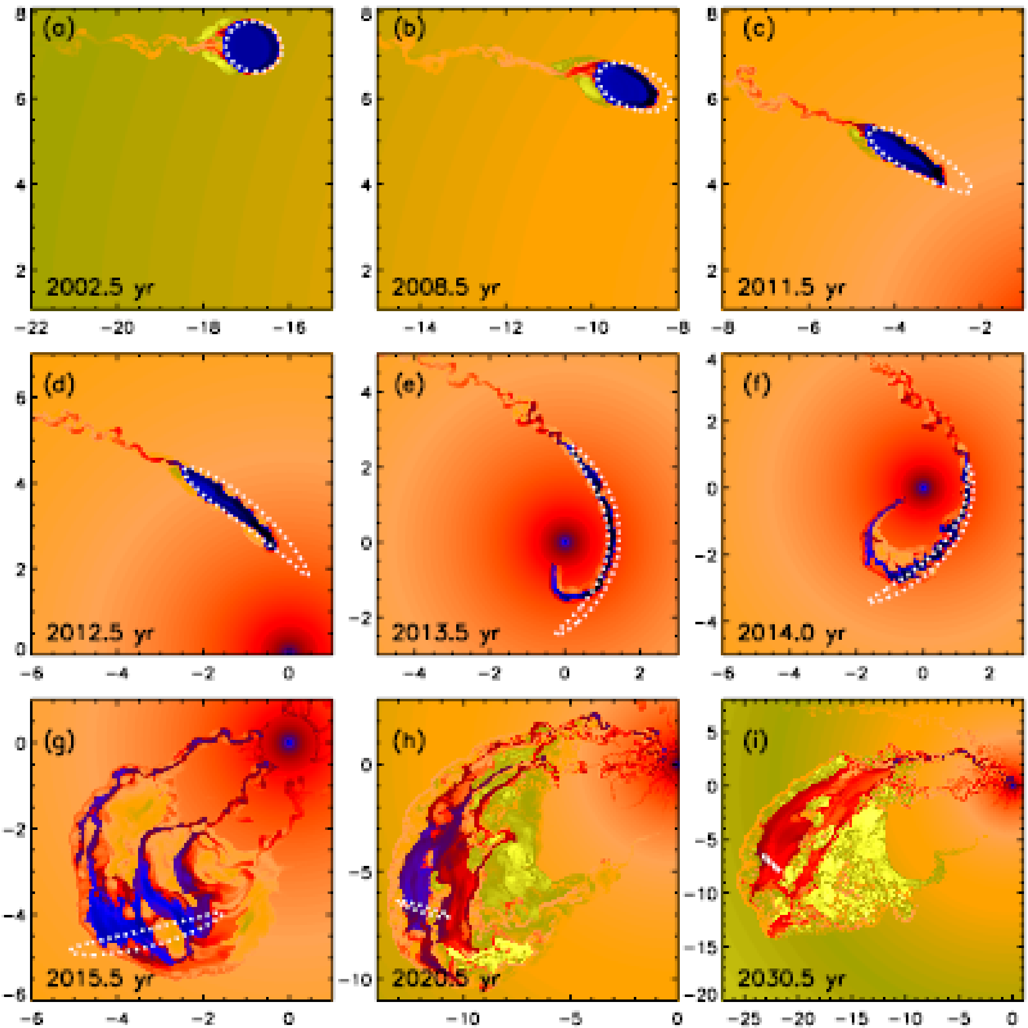

DSO/G2 has survived its closest approach to SgrA*

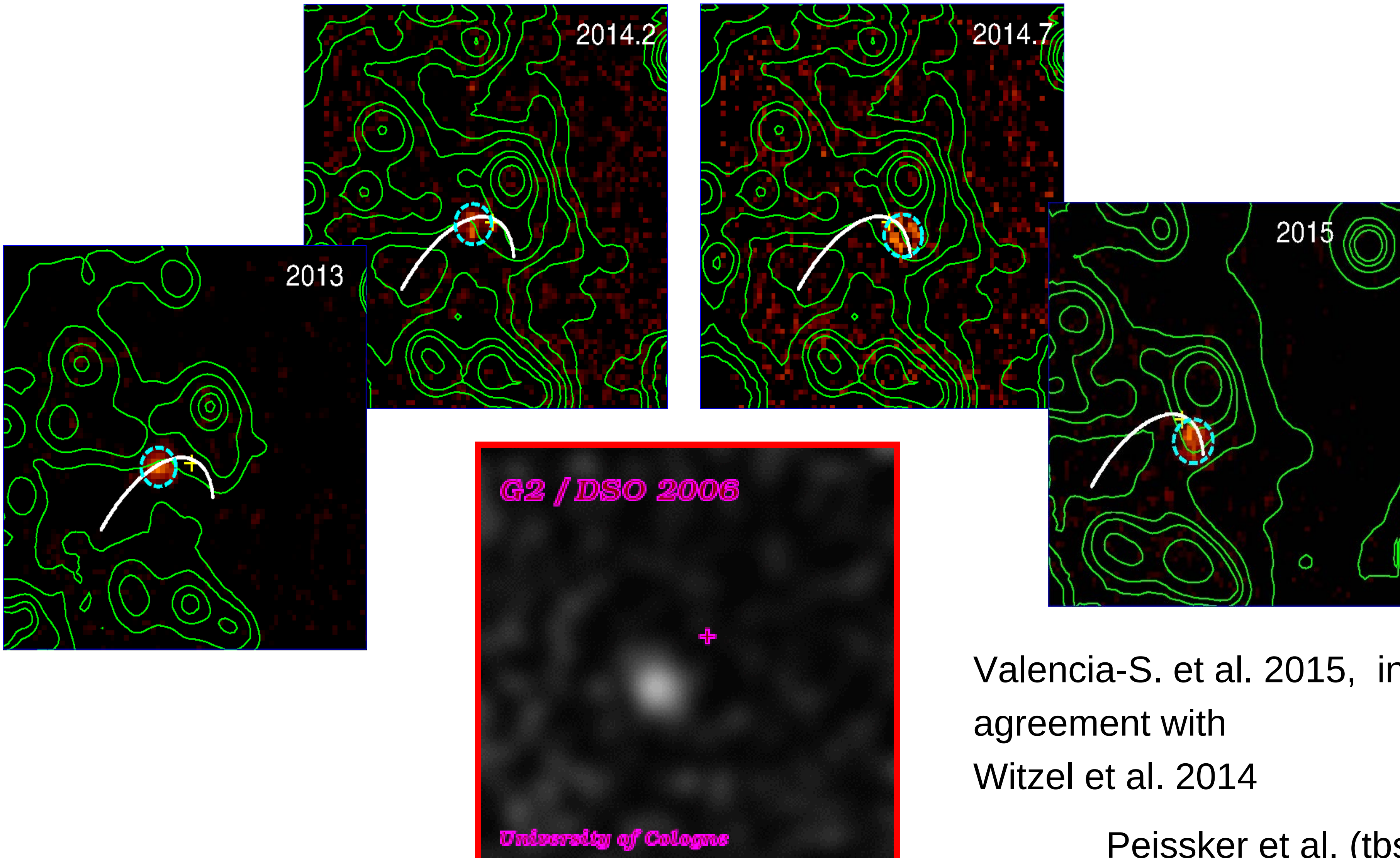

Valencia-S. et al. 2015, in agreement with Witzel et al. 2014

Peissker et al. (tbs)

Brγ line maps of the DSO

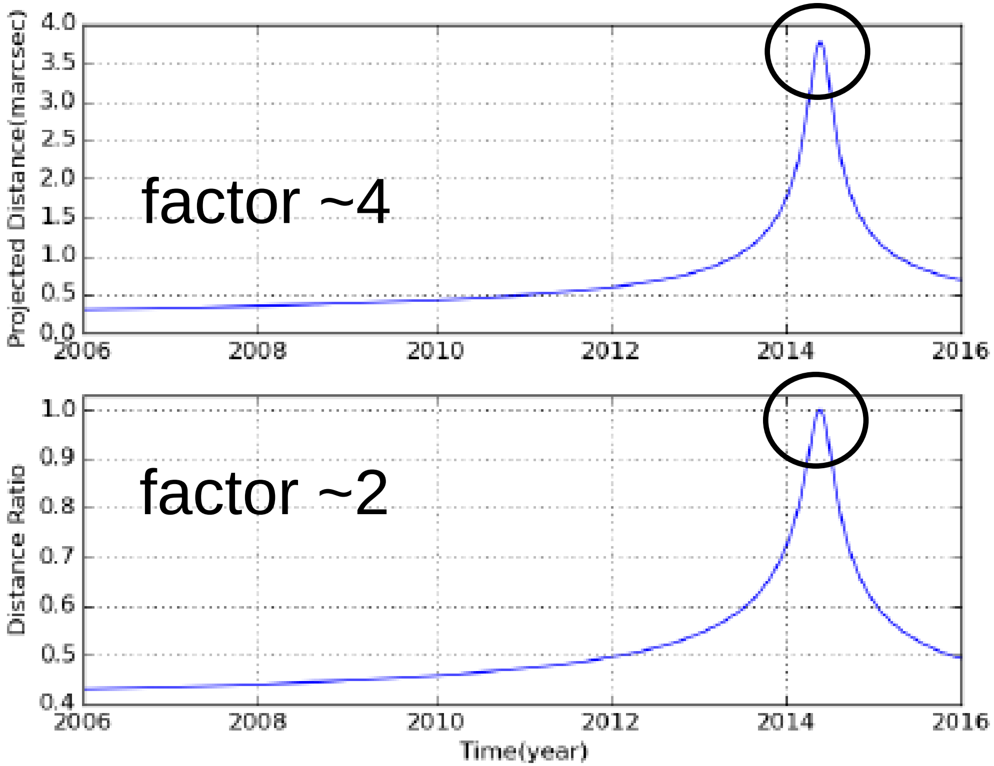

Orbital projection effects: Top: The evolution of the projected separation between two neighboring points of arbitrary 0.5 units in 2011. Bottom: Foreshortening factor of any structure along the orbital extent as a function of time.

During periapse the source is seen at its full size

Both Brγ and L-band continuum originate from a <20mas compact source

Valencia-S. et al. 2015 ApJ

DSO/G2 emits K-band continuum

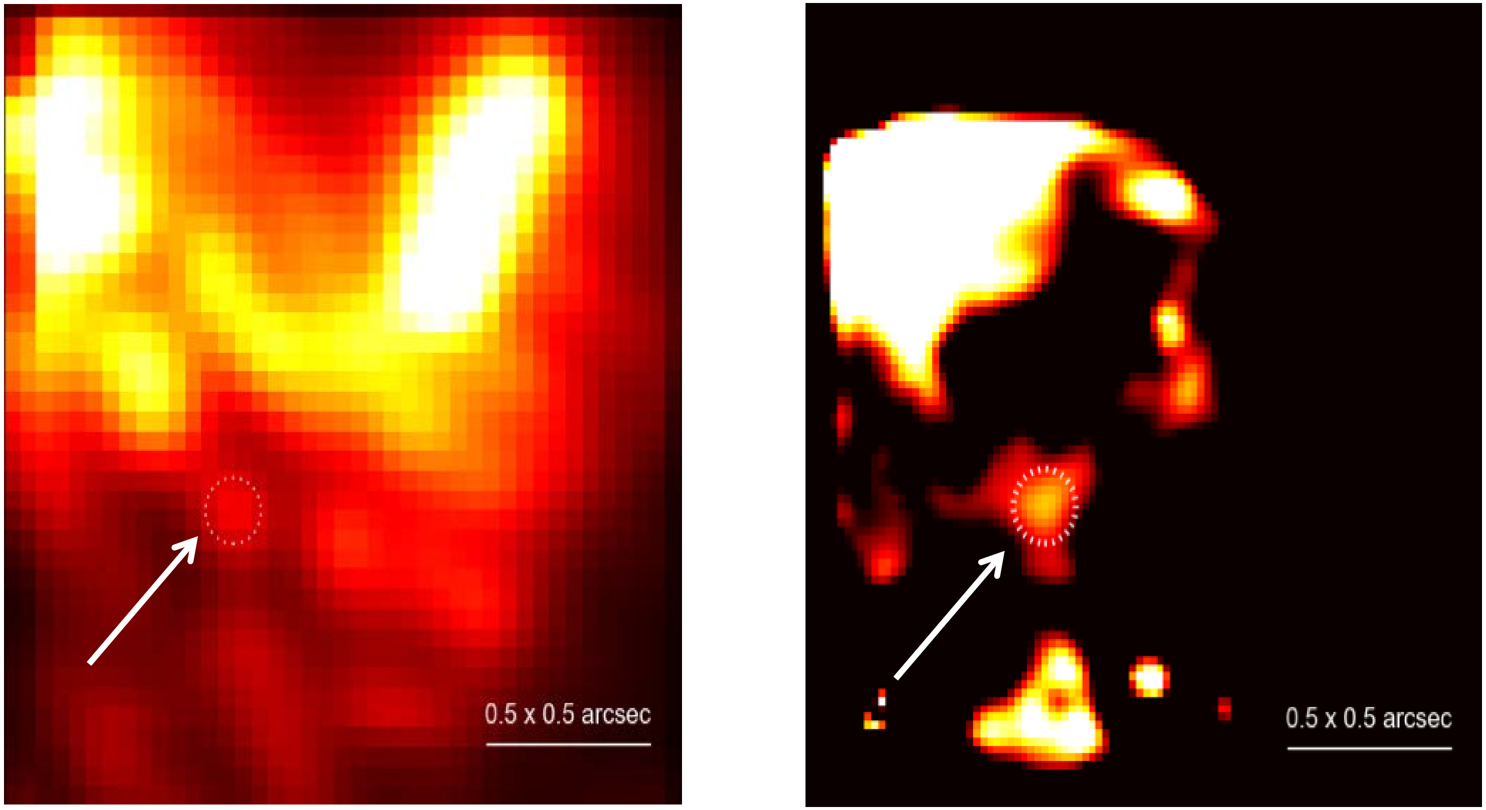

2006-2015 recentered at the DSO position and combined

Eckart et al. 2013

DSO/G2 orbit

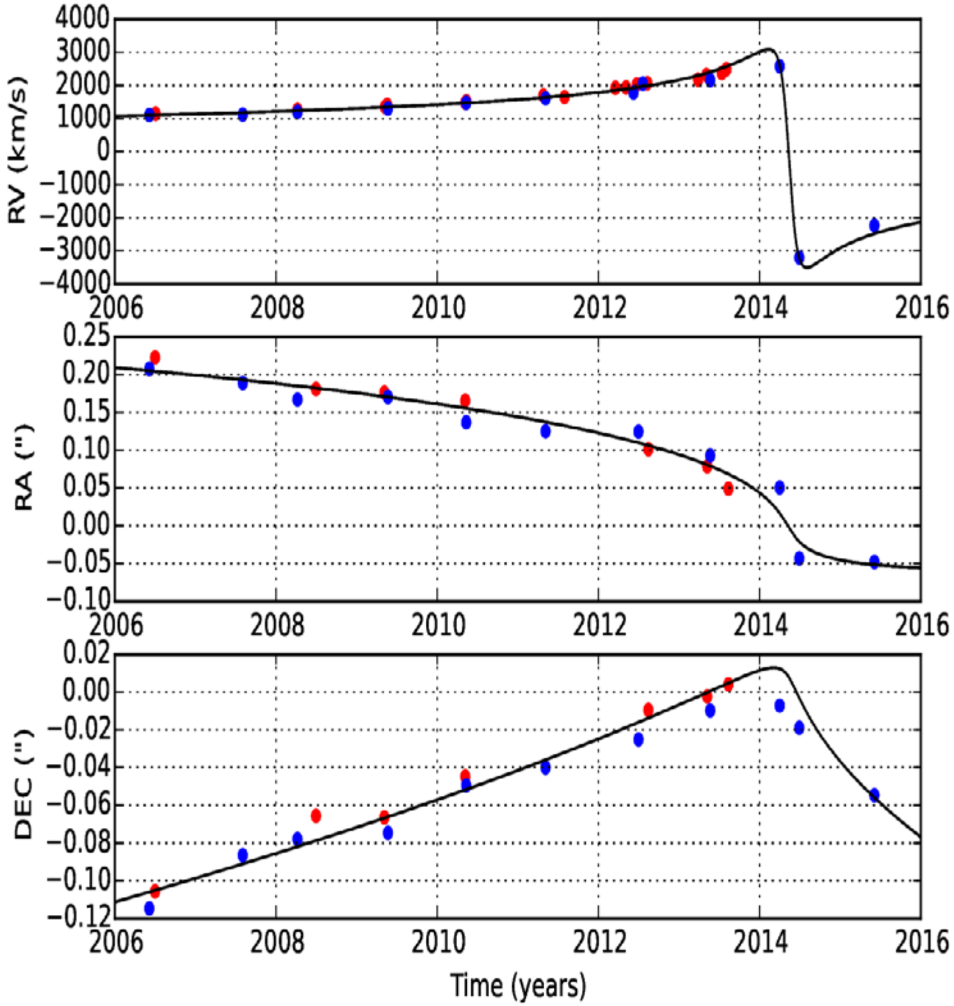

Meyer et al. 2014a,b

Valencia-S et al. 2015
Peissker et al. (tbs)

e=0.976

Pericenter distance: 163 AU

in agreement with Pfuhl et al. 2015; Phifer et al. 2013; Meyer et al. 2014b

Discovery of a new faint Dusty S-cluster member: OS1

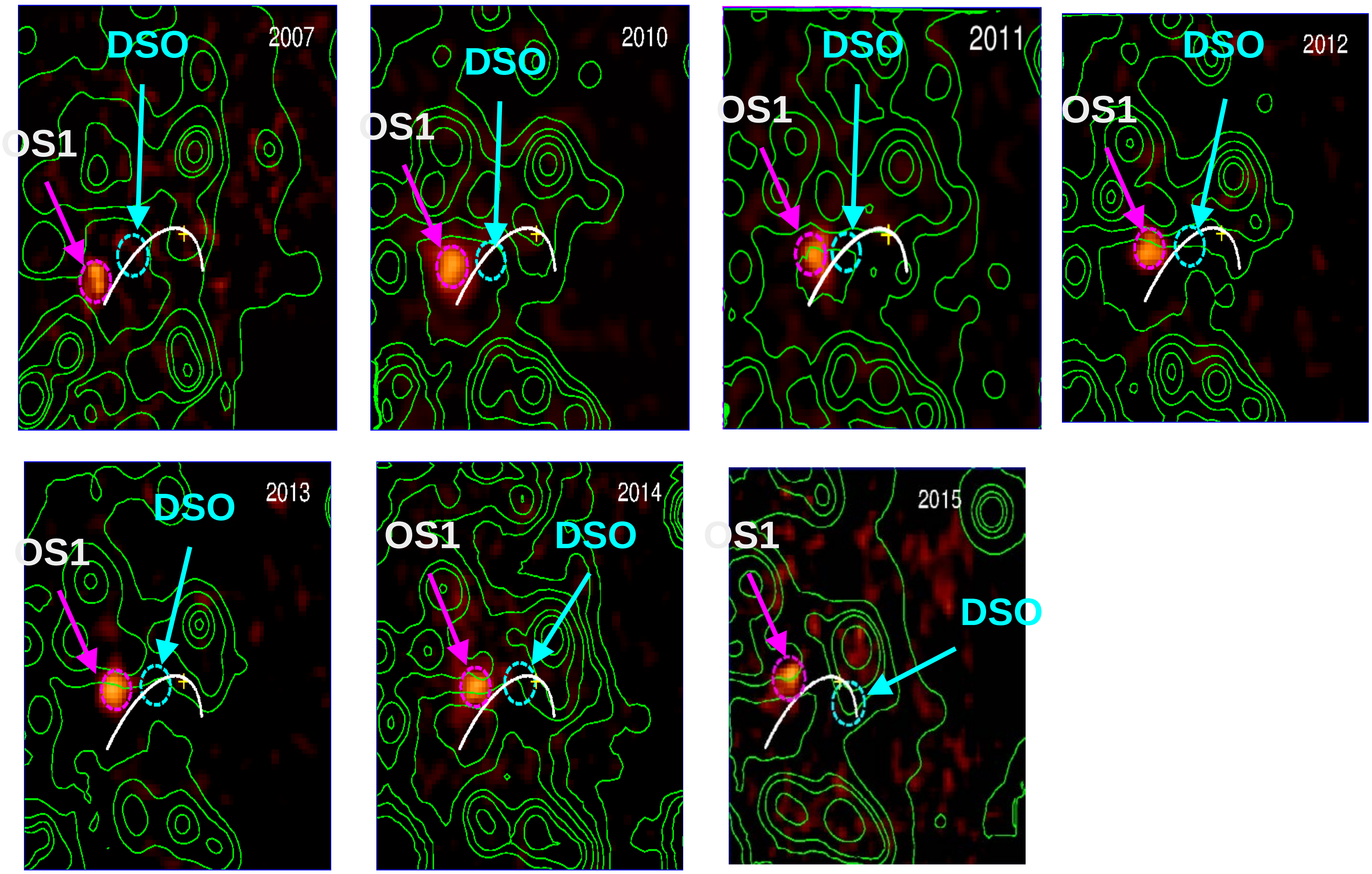

OS1 does not follow the DSO trajectory

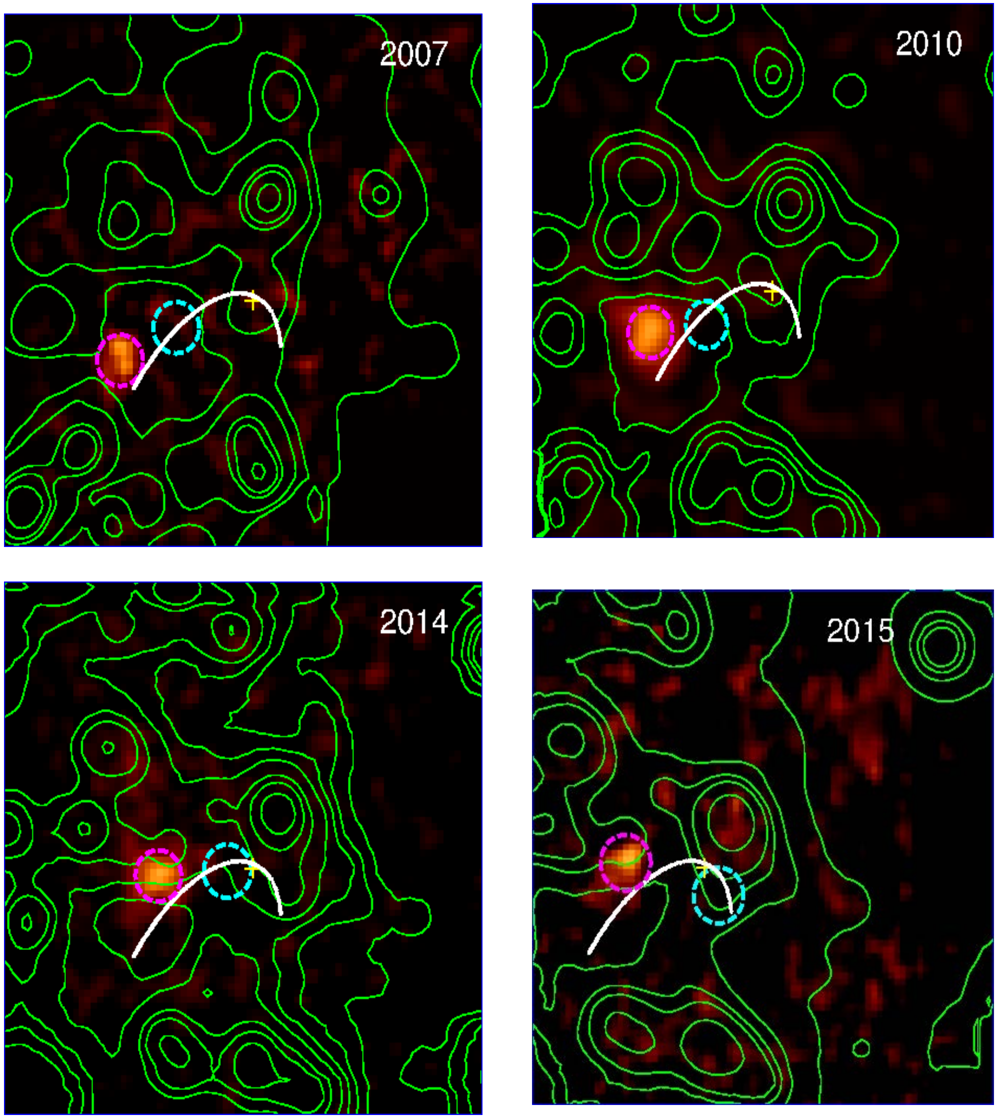

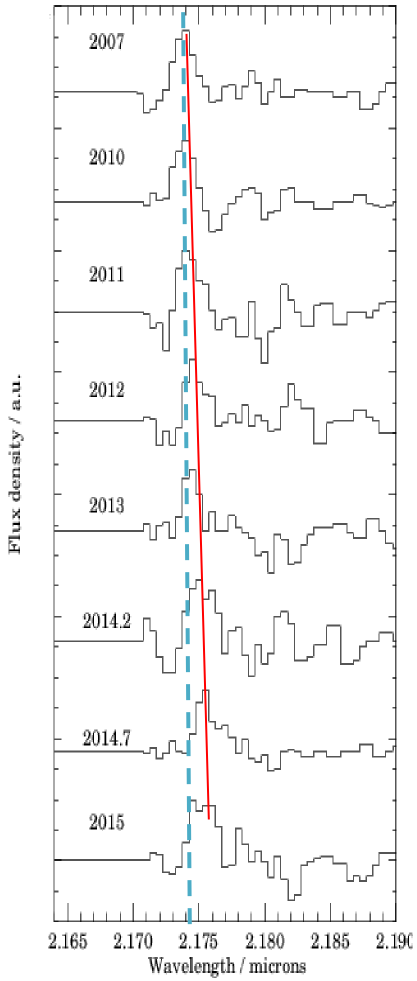

Peissker, Eckart, Valencia-S et al. (tbs)

OS1 does not follow the DSO trajectory

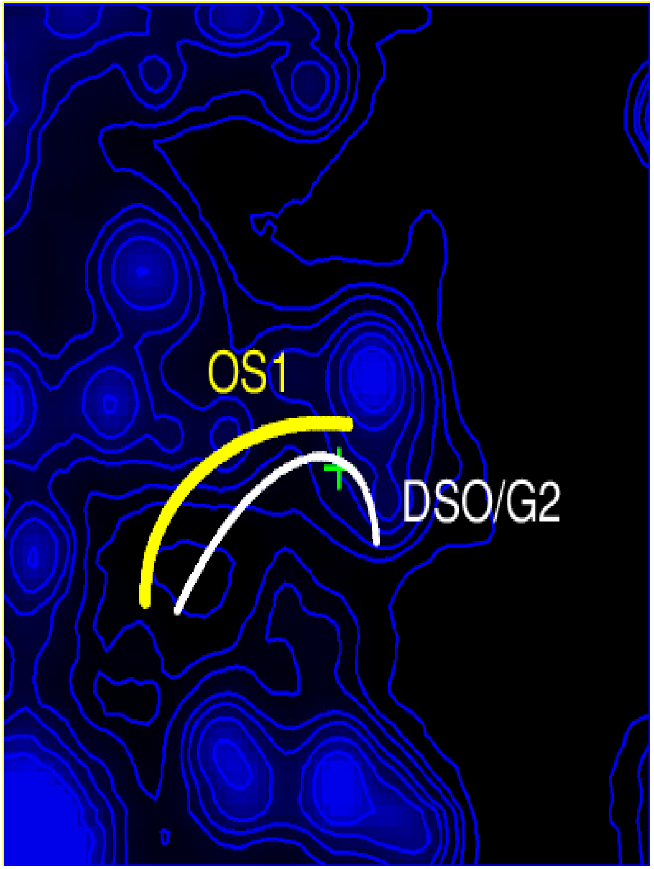

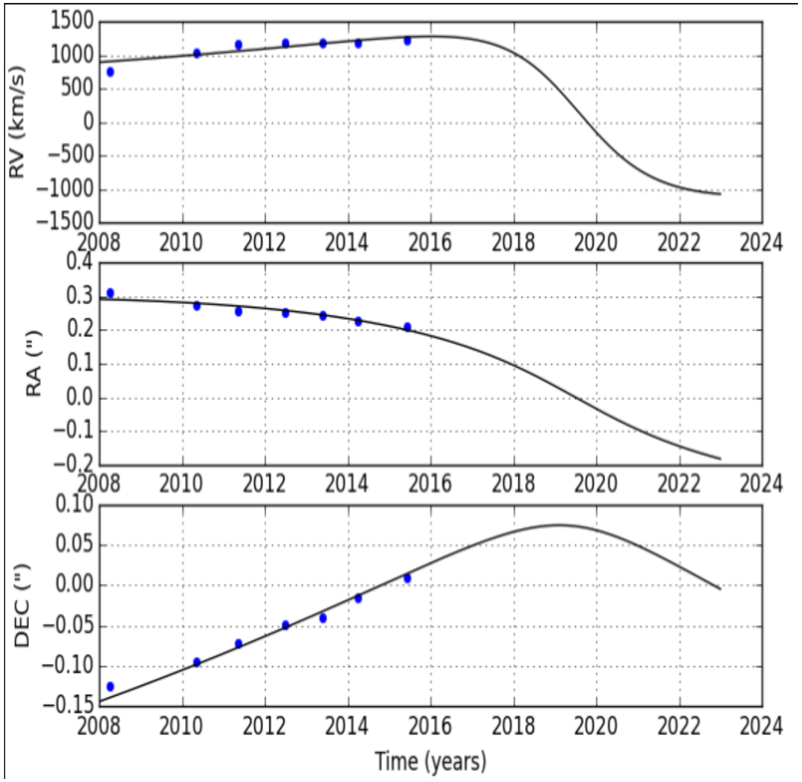

Periapse distance: 750 AU

Peissker, Eckart, Valencia-S et al. (tbs)

Potential reasons for having a large line width

Plus interaction with ambient medium

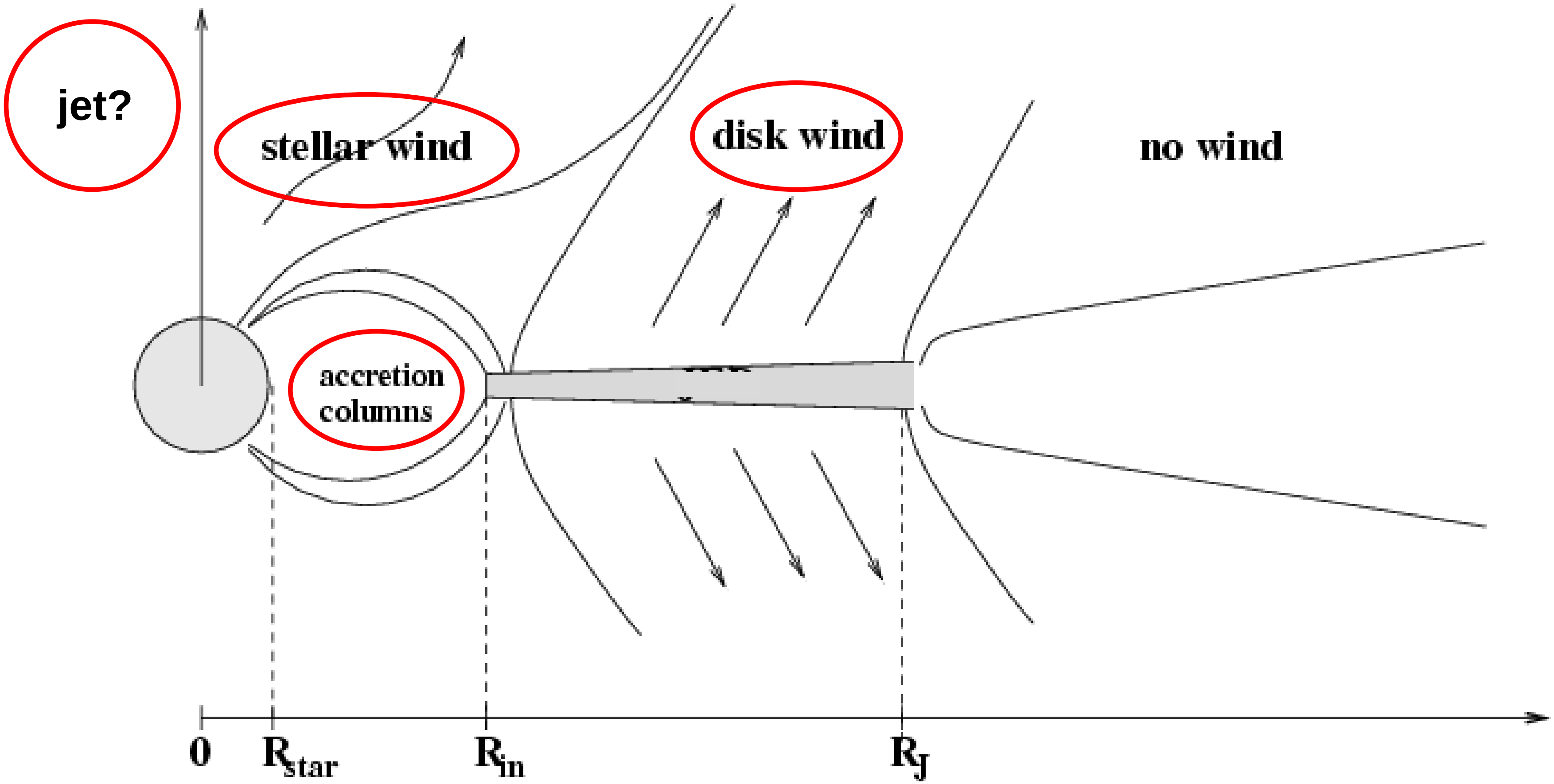

A&A 479, 481-491 (2008)
The radial structure of protostellar accretion disks
C. Combet and J. Ferreira

Pre-main sequence stars with large line widths

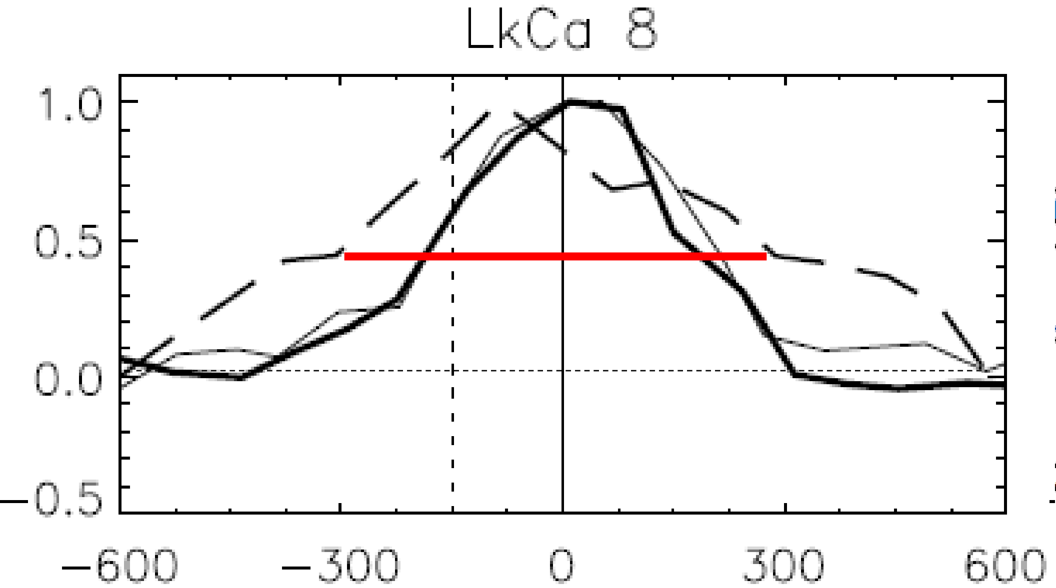

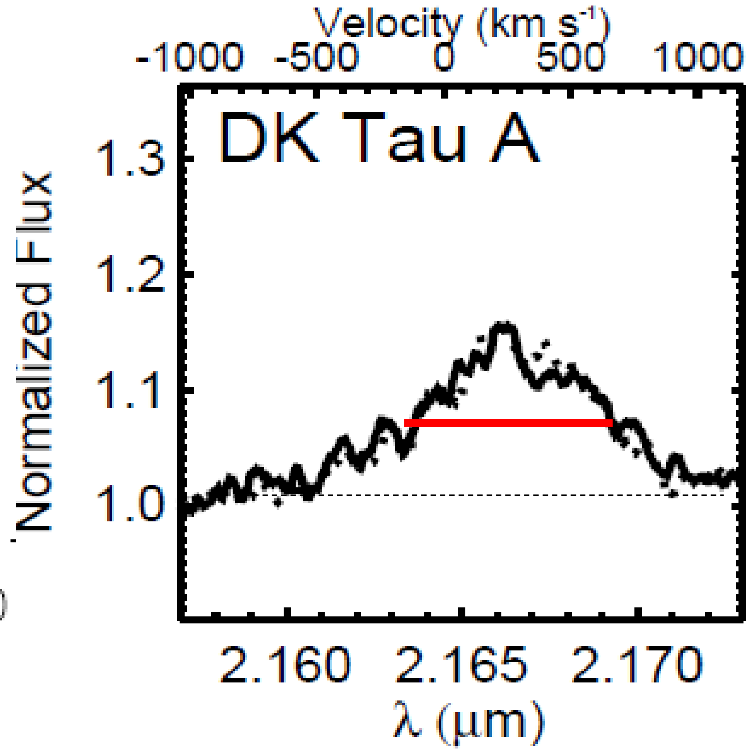

Edwards et al. 2013
M0V ; T Tauri ; around 2 solar masses
600-700 km/s in Brγ

Eisner et al. 2007
Herczeg & Hillenbrand 2014
K8.5 ; 0.68 solar masses
800 km/s in Brγ

DSO/G2 as a young stellar object

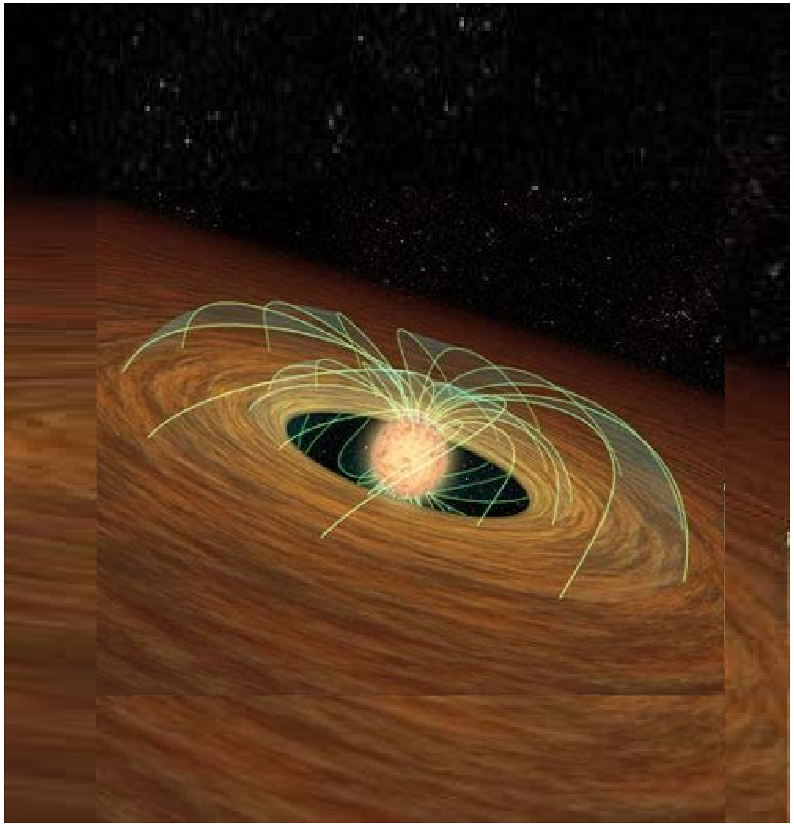

Bry production mechanisms:
Ionized winds, accretion funnel flows, the jet base, bow shock layer

Bry broadening:
Inclination of the system
magnetospheric accretion model (200-700 km/s)

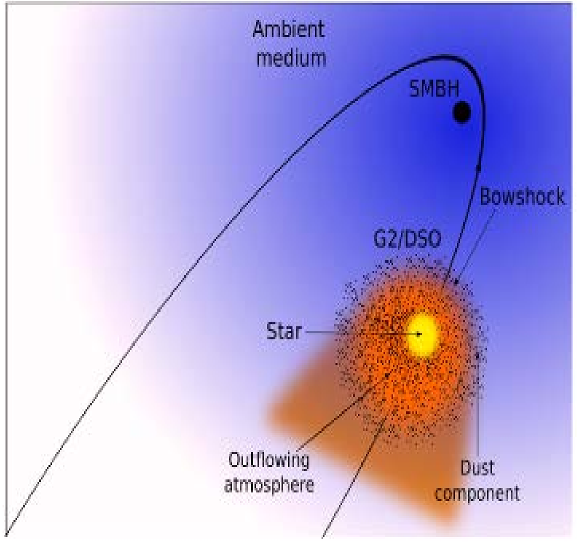

Davies et al. 2011; Rosen, Krumholz, Ramirez-Ruiz, 2012, Eckart et al. 2014

Zajacek, Karas, Eckart 2014

The DSO is polarized in the NIR

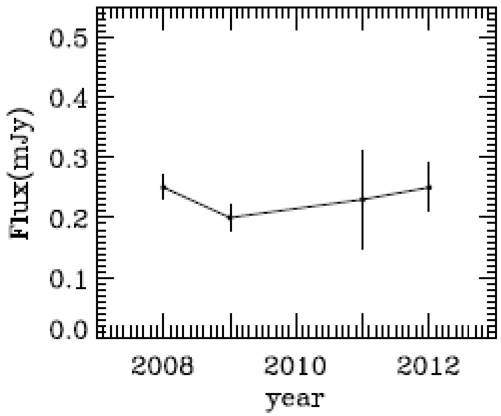

Fig. 2. NIR K_s-band light curve of the DSO observed in polarimetry mode in different years of 2008, 2009, 2011, and 2012.

Shahzamanian et al. 2016

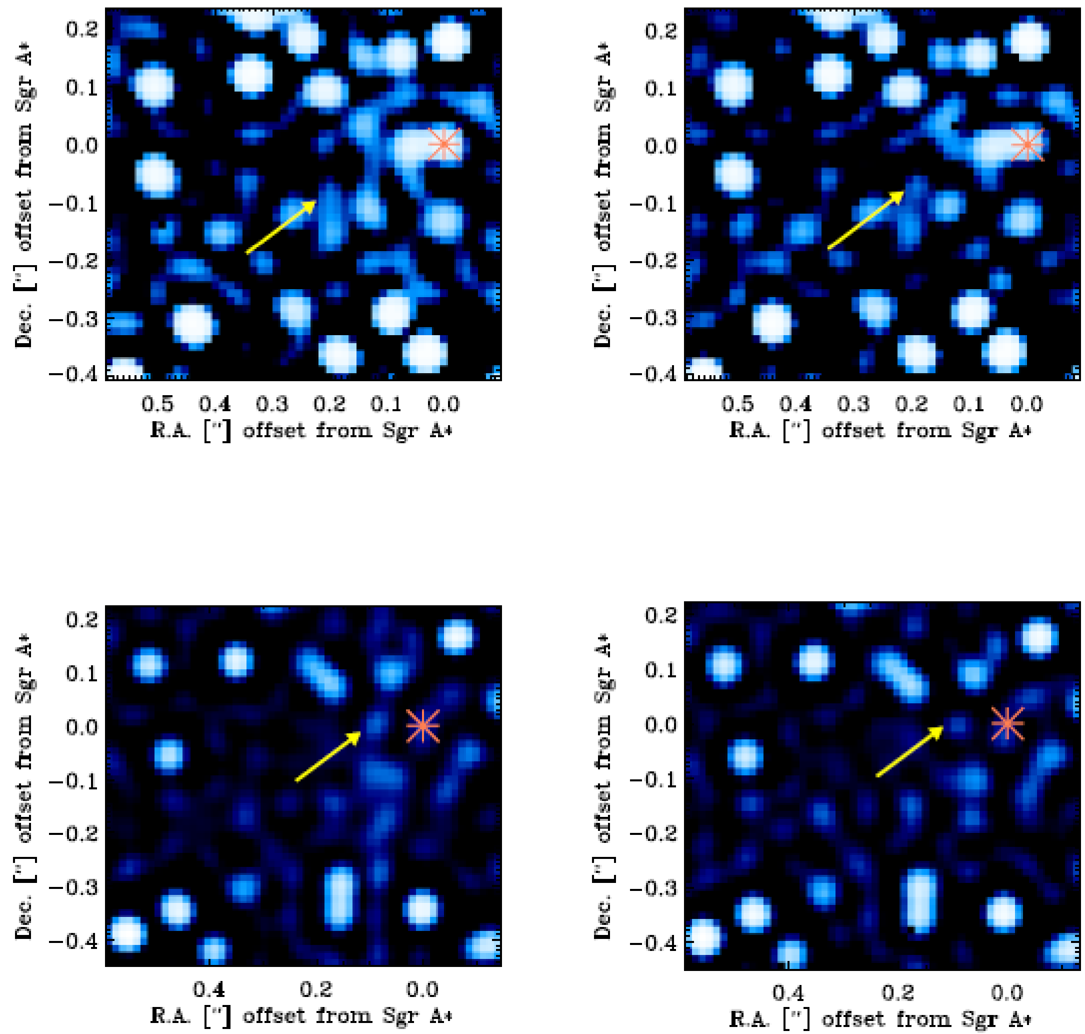

Fig. 1. The final K_s-band deconvolved median images of the central arcsecond at the GC in polarimetry mode (left: 0°, right: 90°) in the years 2008 (top) and 2012 (bottom). The arrow points to the position of the DSO and the asterix indicates Sgr A* position. In all the images North is up and East is left.

The DSO is polarized in the NIR

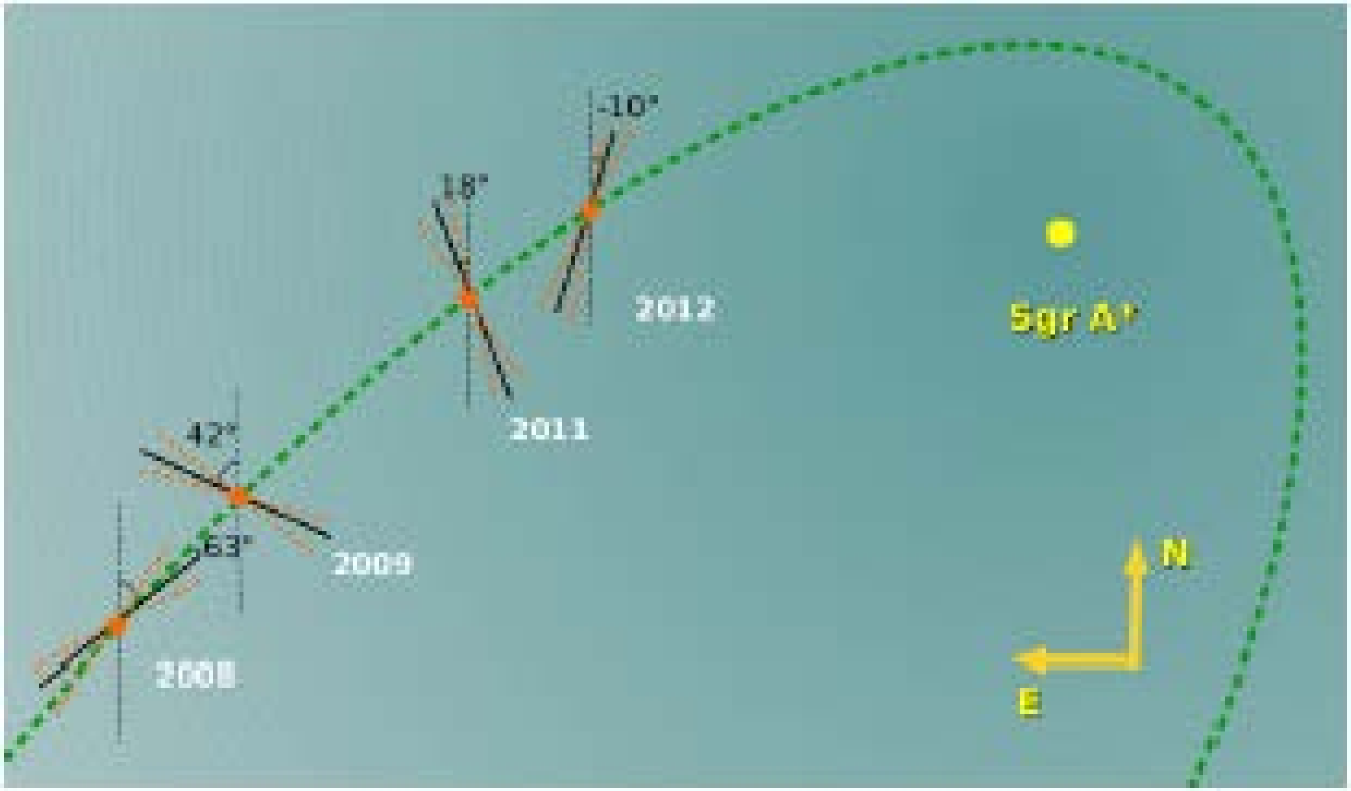

Fig. 3. Sketch of the DSO polarization angle variation when it moves on its eccentric orbit around Sgr A* position for four different years. : this part will change: The orange shaded areas show the range of possible values of polarization angle based on our observation and simulation results.

Shahzamanian et al. 2016

The DSO is polarized in the NIR

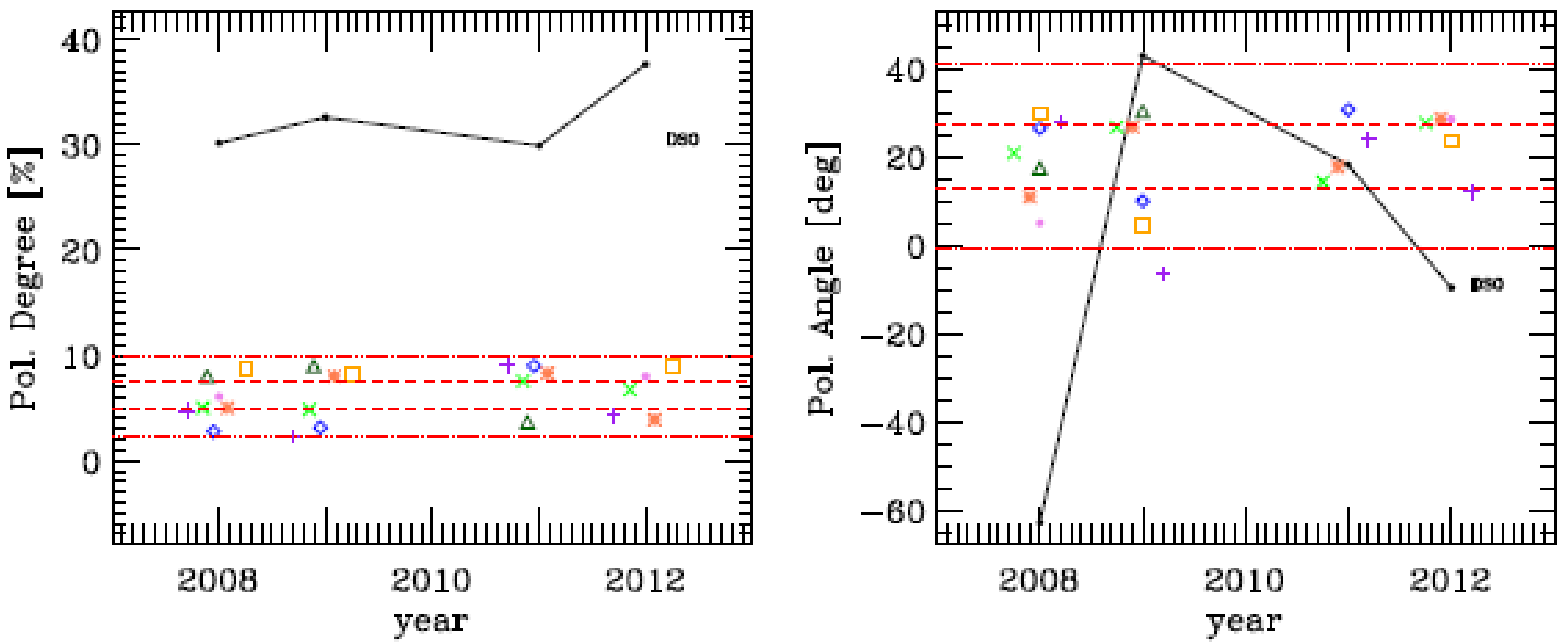

Fig. 4. Left: Comparison of the polarization degree of the DSO (black dots) with the ones of GC S-stars located close to the DSO position (S7, S57, S19, S20, S40, S23, S63). Right: Comparison of the polarization angle of the DSO (black dots) with the ones of the S-stars similar to the left panel. In both panels: Some of the considered stars are not isolated in some years in which it is difficult to calculate their polarization parameters, therefore we didnot show them as data points. The regions between two dashed red lines and dotted lines present the 1 and 3σ confidence intervals of the K_s-band polarization degree and angle distributions of the stars reported in Buchholz et al. (2013), respectively.

Shahzamanian et al. 2016

DSO model: shocked stellar wind

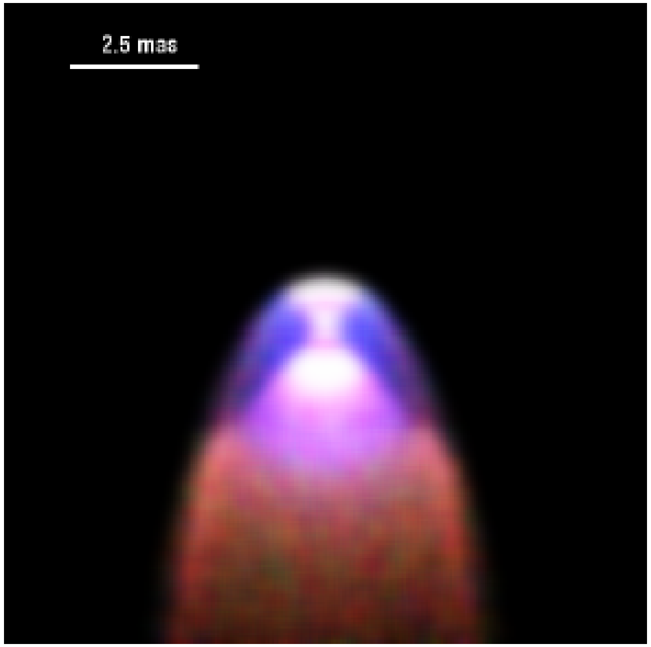

Fig. 9. The RGB image of the source model of the DSO. The explanation is in the text.

Shahzamanian et al. 2016

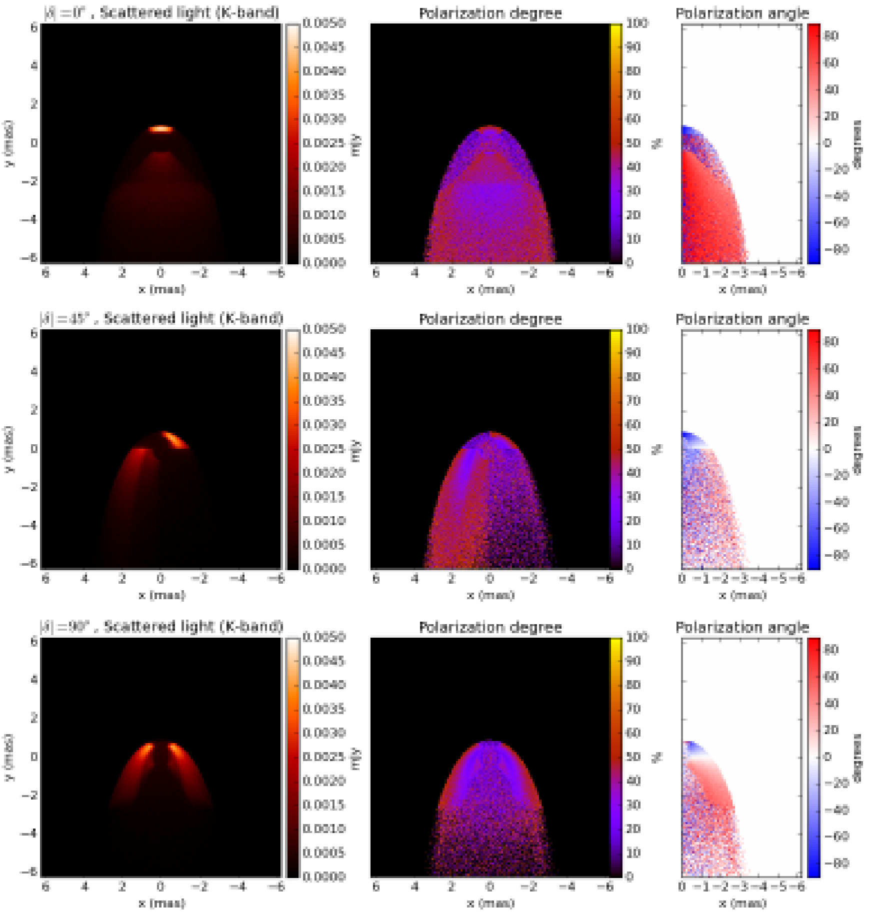

Fig. 8. The emission map of scattered light in K_s band, the distribution of the polarization degree and the angle in the left, middle, and the right panels, respectively for three different configurations of the star–outflow system: $\delta = 0°, 45°, 90°$ from the top to the bottom panels.

General Summary

Experimental Indicators of Accretion Processes in AGN

Starformation and Black Hole Growth jet formation as well as NLR and BLR reverberation indicate compactness and activity of the region around the Black Hole

SgrA* as a special nearby case

NIR polarization of SgrA* over the past ~10 years, as well as radio monitoring indicate that SgrA* is a stabily accreting system
Monitoring the Dusty S-cluster Object

Summary for the DSO

1. DSO/G2 line emission remains compact through the years. DSO/G2 emits K-band continuum emission (18 mag) and has survived the closest approach to SgrA*.
2. DSO/G2 PV diagrams can also capture emission from the fore/background and other line-emitting sources.
3. Discovery of OS1 → Existence of a population of faint, dusty objects.
4. The NIR continuum of the DSO is polarized

- DSO might be a YSO (T Tauri M=0.8-2.0$M_\odot$, ~0.1Myr)

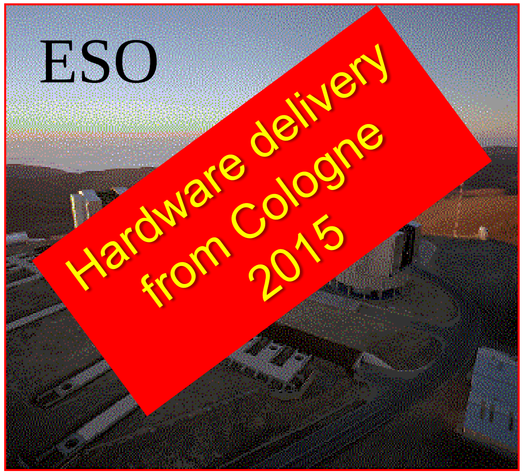

NL leads Euro-Team
Universitity of Cologne
studies for
METIS @ E-ELT

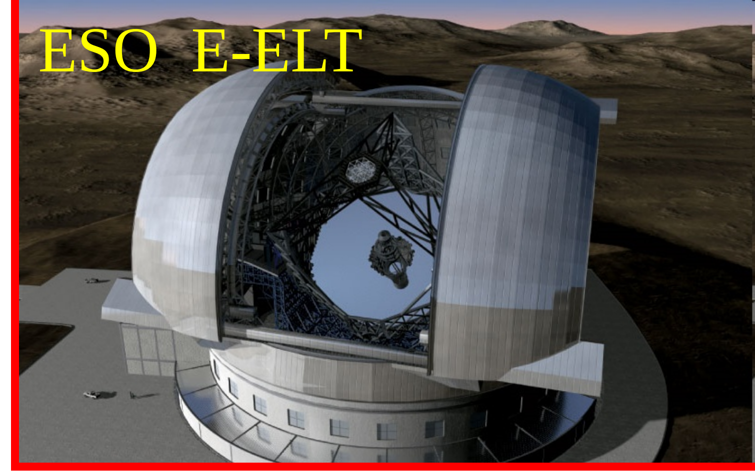

The Galactic Center is a unique laboratory in which one can study signatures of strong gravity with GRAVITY

MPE, MPIA, Paris, SIM
Universitity of Cologne
participation
GRAVITY @ VLTI

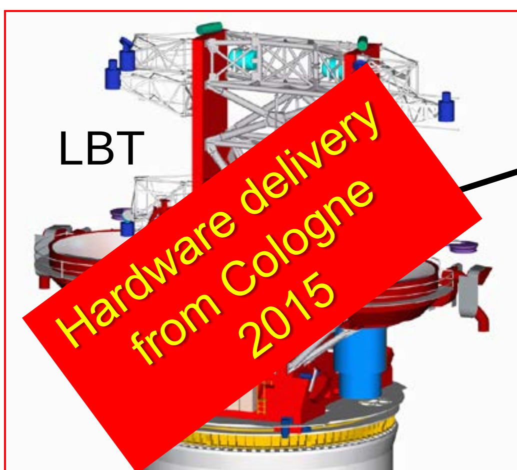

NIR Beam Combiner:
Universitity of Cologne
MPIA, Heidelberg
Osservatorio Astrofisico di Arcetri
MPIfR Bonn

Hardware delivery
from Cologne
2013

Cologne
contribution to
MIRI on JWST

Cologne built Fringe Tracking Spectrometer for GRAVITY

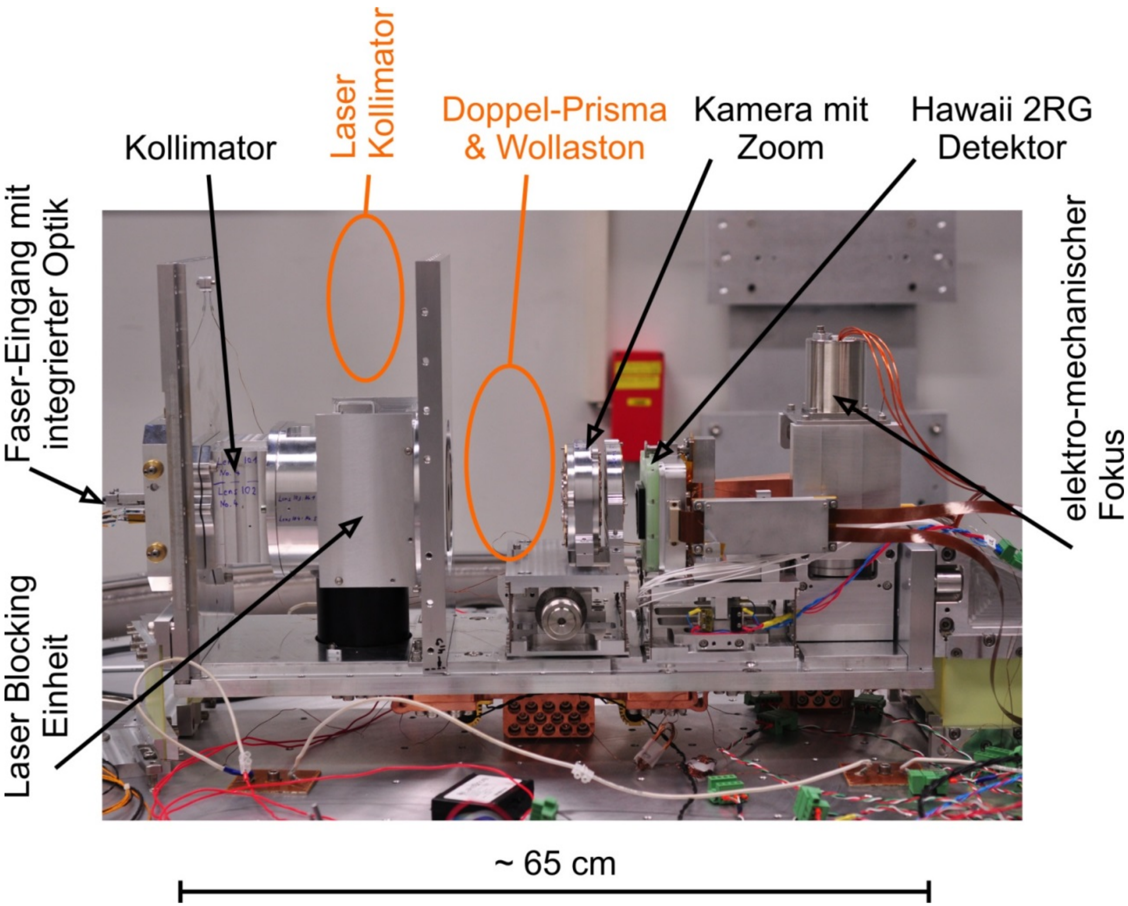

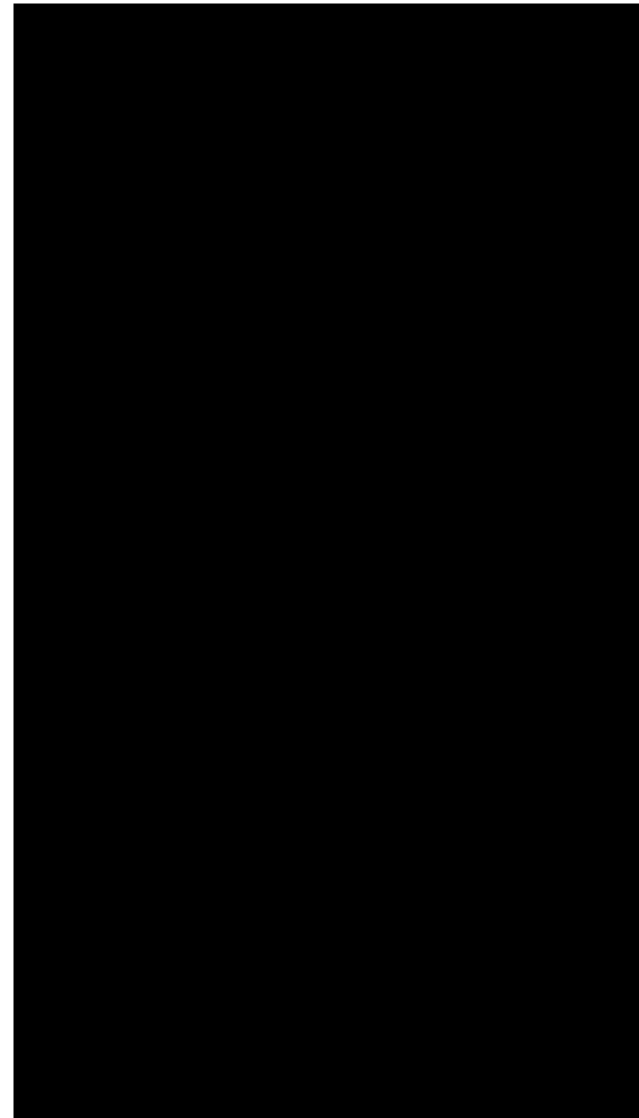

End